

Final Report

Investigation of a Failure of Line 300 at Mile Post 284.14 during Hydrostatic Test 117

MJ Rosenfeld, PE
March 16, 2012



Kiefner & Associates, Inc.
585 Scherers Court
Worthington, Ohio 43085

(614) 888-8220
www.kiefner.com

Intentionally blank

Final Report

on

**INVESTIGATION OF A FAILURE OF LINE 300B AT MILE POST 284.14
DURING HYDROSTATIC TEST 117**

to

PACIFIC GAS & ELECTRIC COMPANY

March 16, 2012

by

MJ Rosenfeld, PE

**Kiefner and Associates, Inc.
585 Scherers Court
Worthington, Ohio 43085**

0215-1116

DISCLAIMER

This document presents findings and/ or recommendations based on engineering services performed by employees of Kiefner and Associates, Inc. The work addressed herein has been performed according to the authors' knowledge, information, and belief in accordance with commonly accepted procedures consistent with applicable standards of practice, and is not a guaranty or warranty, either expressed or implied.

The analysis and conclusions provided in this report are for the sole use and benefit of the Client. No information or representations contained herein are for the use or benefit of any party other than the party contracting with KAI. The scope of use of the information presented herein is limited to the facts as presented and examined, as outlined within the body of this document. No additional representations are made as to matters not specifically addressed within this report. Any additional facts or circumstances in existence but not described or considered within this report may change the analysis, outcomes and representations made in this report.

TABLE OF CONTENTS

INTRODUCTION	1
SUMMARY AND CONCLUSIONS.....	1
BACKGROUND.....	2
INVESTIGATION.....	2
Visual Examination.....	2
Fractographic Examination.....	5
Visual Examination.....	5
Microscopic Examination	6
Scanning Electron Microscope Examination	9
Metallographic Sections.....	18
Material Properties	20
Tensile Tests	20
CVN Impact Tests.....	21
Material Chemistry	25
DISCUSSION	26
The Hot Crack.....	26
The Lack of Penetration.....	27
Fracture Assessment	27
APPENDIX A: OTHER IMPERFECTIONS ON SAMPLE PIPE	29
Longitudinal Seam Repairs.....	29

LIST OF FIGURES

Figure 1. Failure Specimen, Coating Removed, Marked for Cutting (photo by author)	3
Figure 2. Reduced Size Specimen Containing Fracture (photo by author)	3
Figure 3. Coupons of Mating Fracture Segments Containing Apparent Origin (photo by author)	4
Figure 4. Composite of Origin, North Fracture Surface, Before Cleaning, 2X (photo by author)	5
Figure 5. Composite of Origin, North Fracture Surface, After Cleaning, 2X (photo courtesy Exponent).....	6
Figure 6. Fracture Surface Before Cleaning, 5X (photo by Exponent)	7
Figure 7. Terminations of Origin Defect, North Fracture Surface, 5X (photo by Exponent)	7
Figure 8. Radial Dimensions of Fracture Features	8

Figure 9. Ratio of Flaw Depth to Metal Thickness.....	8
Figure 10. Zone 1 and Upper Part of Zone 2, 25X.....	10
Figure 11. Detail in Zone 1, 500X.....	10
Figure 12. Zone 2 Surface, 100X.....	11
Figure 13. Detail of Zone 2, 1,000X.....	11
Figure 14. Local Extension of Zone 2 to Exterior Surface, 20X.....	12
Figure 15. Detail at Edge of Zone 1 Extension, 400X.....	12
Figure 16. Zone 3 Surface, 25X.....	13
Figure 17. Detail of Zone 3, 500X.....	13
Figure 18. Zone 4 between Lower Part of Zone 3 and Upper Part of Zone 5, 25X.....	14
Figure 19. Detail of Zone 4, 350X.....	14
Figure 20. Detail of Zone 4, 500X.....	15
Figure 21. Zone 5 Surface, 25X.....	15
Figure 22. Detail of Zone 5, 100X.....	16
Figure 23. Zone 6 at Bottom of Zone 5, 25X.....	16
Figure 24. Detail of Zone 6, 500X.....	17
Figure 25. Metallographic Cross Section, Mount A, 5X.....	19
Figure 26. Metallographic Cross Section, Mount B, 5X.....	19
Figure 27. Intact Seam Showing Normal Seam Weld Deposition.....	20
Figure 28. CVN Test Results for Seam Weld Specimens.....	23
Figure 29. CVN Test Results for Pipe Body Specimens.....	24
Figure 30. Seam Weld Repair, T117-CE-LS-E, Interior Surface.....	29
Figure 31. Seam Repair, T117-CE-LS-E, Section A.....	30
Figure 32. Seam Repair, T117-CE-LS-W, Section B.....	30
Figure 33. Seam Repair, T117-CE-LS-W, Interior Surface.....	31
Figure 34. Seam Repair, T117-CD-LS-W, Section A.....	31
Figure 35. Hot Crack, T117-CC-T-W (25X).....	32
Figure 36. LOP Feature, T117-CC-T-W (50X).....	32
Figure 37. Surface Imperfection, T117-CE-LS-W.....	33
Figure 38. Surface Imperfection, Metallographic Section.....	33

LIST OF TABLES

Table 1. Fracture Zones Identified by SEM.....	9
Table 2. Tensile Testing Results.....	21
Table 3. CVN Specimen Test Temperatures	22
Table 4. Interpreted CVN Test Results.....	25
Table 5. Material Chemistry Data.....	26

Intentionally blank

Investigation of a Failure of Line 300B at Mile Post 284.14 during Hydrostatic Test 117

MJ Rosenfeld, PE

INTRODUCTION

Pacific Gas & Electric Company (PG&E) is performing hydrostatic pressure tests of its Line 300B in order to revalidate the established maximum allowable operating pressure (MAOP). A failure occurred in the line at Mile Post 284.14 during Test 117. A metallurgical investigation was performed by PG&E. PG&E requested the participation of outside technical consultants consisting of Dr. Brad James of Exponent, Inc. and also the author. The Consumer Protection and Safety Division (CPSD) of the California Public Utility Commission (CPUC) was actively represented by Mr. Sunil Shori throughout all phases of the investigation. This report documents the author's observations, interpretations, and conclusions made during the investigation.

SUMMARY AND CONCLUSIONS

The failure originated at a hot crack in the outside pass of the double submerged-arc weld (DSAW) longitudinal seam. The hot crack was approximately 6.5 inches long and extended radially through most of the outer weld deposit. The reason for the formation of this particular hot crack is unknown, but two factors may have played a role. One is that historical inspections of pipe produced by Consolidated Western have indicated a tendency for hot cracking to occur at the pipe ends due to insufficient restraint of elastic springing of the pipe in their welding fixtures. Although this crack did not occur precisely at the end of the pipe, it was located within 1.5 ft of the end and could have been influenced by end restraint conditions. Second, the chemistry of the base metal exceeded an empirical threshold indicating low resistance to hot cracking, although the chemistry was very typical for pipe of the designated grade and vintage.

The hot crack occurred coincidentally with a lack of penetration (LOP) between the inner and outer weld deposits. The LOP was due to lateral offset of the outer weld pass such that the points of maximum penetration of the inner and outer weld deposits did not coincide with each other, leaving the abutting plate edges unfused at mid-wall-thickness. The LOP condition extended upstream and downstream of the hot crack and would not have been detectable by visual inspection or by hydrostatic pressure testing to prescribed pressure test levels. The failure occurred due to the coincidental occurrence of the hot crack and LOP together. Either feature acting alone would have survived the hydrotest.

The hot crack was an original manufacturing defect which survived the hydrostatic pressure test conducted by the pipe manufacturer at the mill. Analysis considering the measured seam strength properties and the observed flaw dimensions indicates that it is reasonable that this flaw survived the mill test.

The hot crack and LOP exhibited no evidence of enlargement in service, e.g. due to fatigue crack growth. The combined defect exhibited small amounts of ductile flaw growth under hydrostatic test conditions immediately prior to the test failure.

BACKGROUND

PG&E is performing hydrostatic pressure tests of its Line 300B in order to revalidate the established maximum allowable operating pressure (MAOP). A failure occurred in the line at Milepost 284.14, Station 14+75, during Test 117. The failure occurred in the longitudinal seam of a pipe that was part of a factory double joint.

The pipe was manufactured in 1949 by Consolidated Western to PG&E Specification PGE-7. The specified dimensions were 34-inch OD x 11/32-inch (0.344-inch) WT. The specified minimum yield strength (SMYS) and specified minimum tensile strength (SMTS) were 52 ksi and 72 ksi, respectively. The mill test pressure specified by PGE-7 was 945 psig corresponding to a nominal hoop stress of 90% of SMYS, which exceeded the minimum mill test to 85% SMYS required by API 5LX at that time. The maximum allowable operating pressure (MAOP) was 757 psig corresponding to a nominal hoop stress of 37,410 psi or 71.94% SMYS.

The test pressure at the time and location of the failure was 998 psig, corresponding to a nominal hoop stress of 49,320 psig or 94.85% SMYS. The pressure at the time of failure was the highest that the pipe had experienced.

INVESTIGATION

Visual Examination

A nominal 40-ft (39-ft, 7-in actual) section centered on the fracture was removed by PG&E and shipped to the PG&E Applied Technical Services facility in San Ramon, CA for initial examination. An overall view of the pipe specimen is shown in Figure 1, viewed looking downstream approximately East to West. Most of the hot applied asphalt coating had been removed except immediately adjacent to the fracture. Slit rubber hoses were placed over the fracture surfaces for mechanical protection. The white lines mark where the specimen was cut to smaller size.

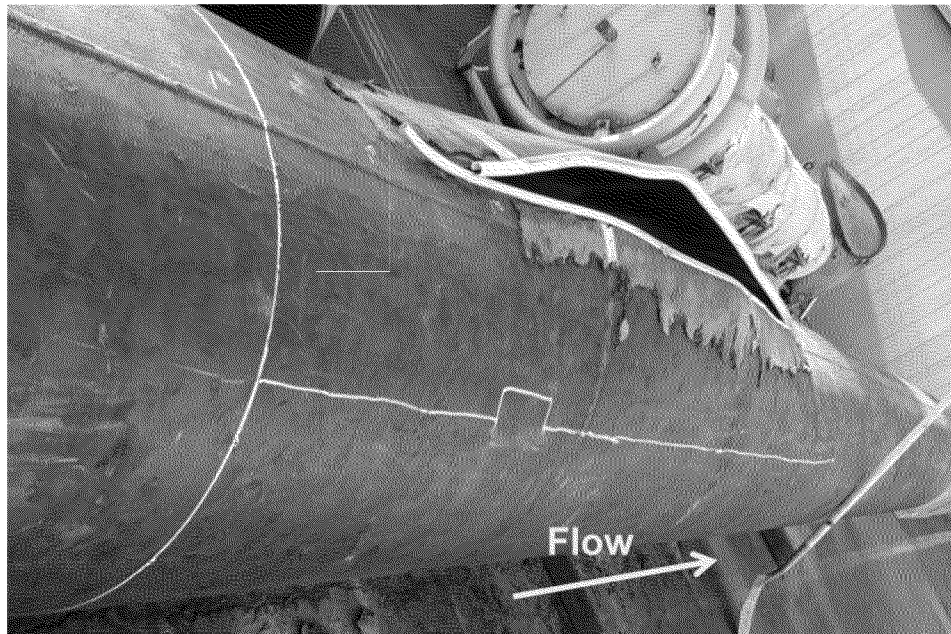


Figure 1. Failure Specimen, Coating Removed, Marked for Cutting (photo by author)

The failure specimen was cut down to manageable size, shown in Figure 2, with remaining coating removed and as marked for further subdivision. The total length of the fracture was 89.5 inches. The fracture intersected a girth weld visible to the right of the locating notch, terminating 19 inches into the upstream pipe joint.

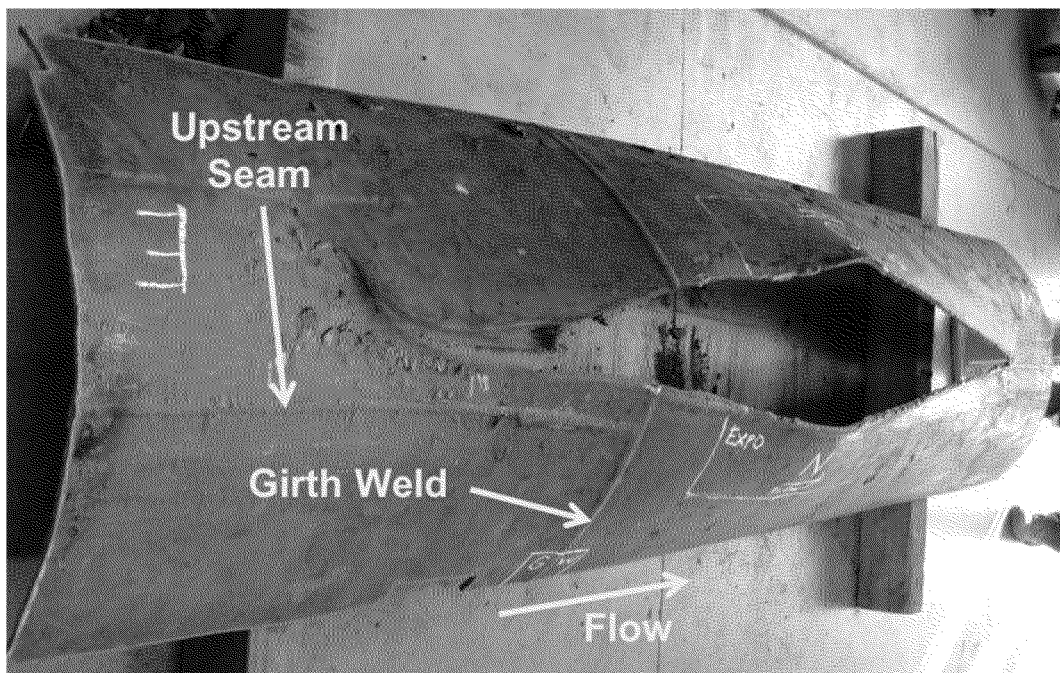


Figure 2. Reduced Size Specimen Containing Fracture (photo by author)

An apparent origin 6.5 inches long was located 14.5 inches downstream of the girth weld. Coupons containing only the central portion of the fracture were cut out to isolate the apparent origin, identified in Figure 3. The apparent origin was confirmed as the probable origin based on its occurrence at the widest point of opening in the rupture, and by the appearance of brittle fracture chevrons in the propagating fracture, which pointed toward the 6.5-inch-long feature.

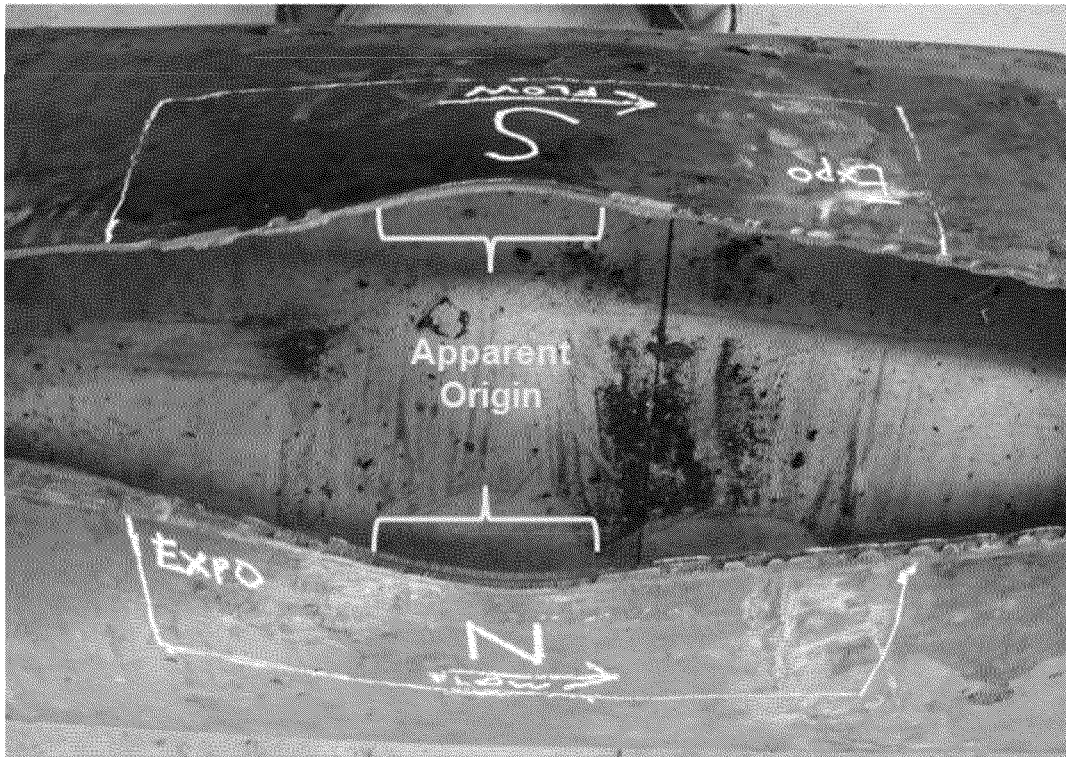


Figure 3. Coupons of Mating Fracture Segments Containing Apparent Origin (photo by author)

The coupons shown in Figure 3 were further examined and tested at the facilities of Exponent, Inc. The results of the examinations and tests are discussed below.

In addition to examination of the apparent origin described above, nondestructive examination of the rest of the pipe performed at PG&E's facility identified minor imperfections in the seam weld and pipe body. Although they were not involved in the test failure, the minor imperfections were also cut out for further examination at Exponent. The results of these examinations are in Appendix A. The examination of the pipe revealed no significant flaws in the form of corrosion or mechanical damage.

Fractographic Examination

Visual Examination

A composite detail of the origin in the condition as discovered is shown in Figure 4 prior to cleaning. The apparent origin is seen to consist of a 6.5-inch-long crack in the outer seam weld deposit. The apparent origin presented a columnar texture typical of certain types of weld cracks, and a dark coloration that could be a stain or oxide. The vertical dashed line in represents match points in the two photos.

An unfused region was present along the center of the weld between the inner and outer seam weld deposits. The dark coloration on the weld crack extended to the unfused region between the weld beads but only over a length essentially coincident with the weld crack. The unfused region extended the full length of the fracture, but did not exhibit the dark coloration beyond the length adjacent to the weld crack. The inner weld deposit exhibited a bright fracture surface consistent with recent brittle fracture. Beyond the 6.5-inch-long defect, the fracture exhibited brittle fracture propagation chevrons that pointed toward the 6.5-inch defect and beyond that transitioning to ductile shear fracture propagation.

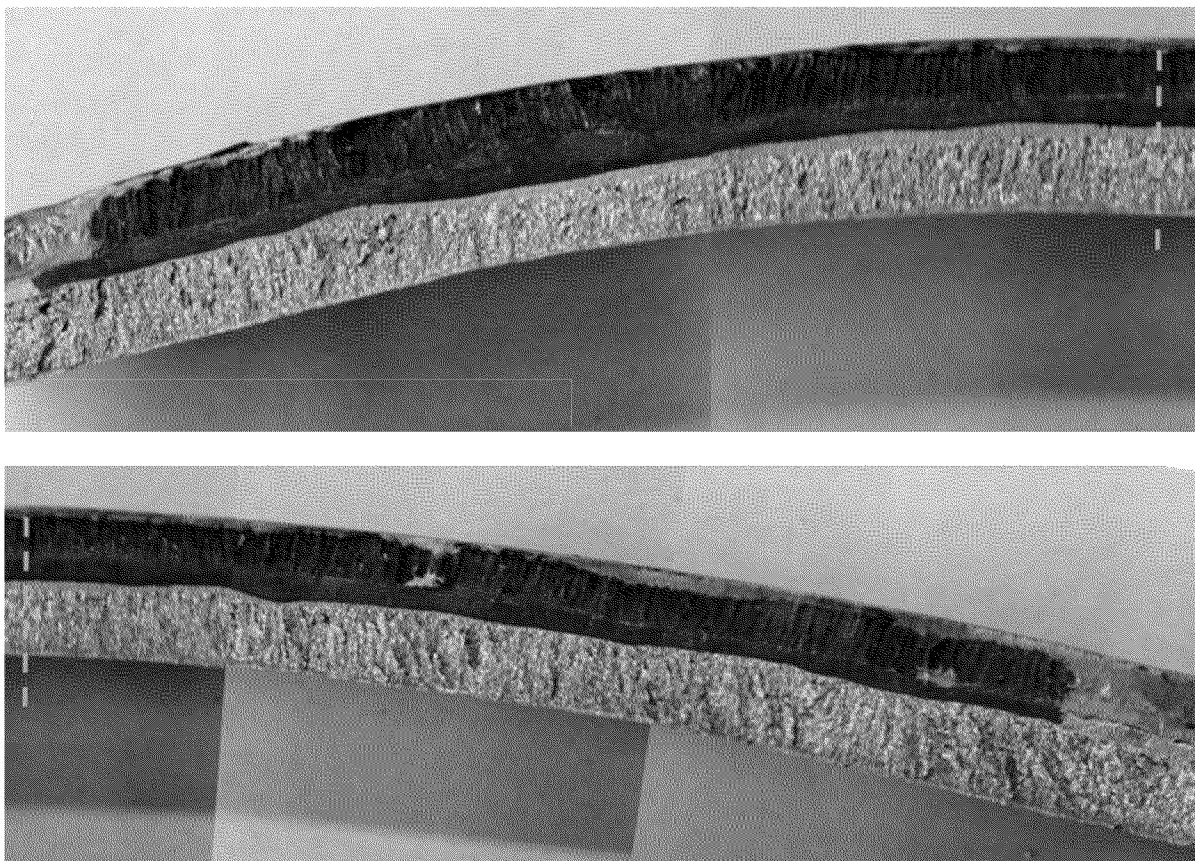


Figure 4. Composite of Origin, North Fracture Surface, Before Cleaning, 2X (photo by author)

The fracture surface was cleaned in acetone, then xylene, and then a nonoxidizing detergent (Alconox). It was then cleaned ultrasonically in a mild alkaline detergent (Micro 90). The cleaning steps failed to remove the dark coloration on the weld crack, but lightened the coloration on the unfused surfaces, as shown in Figure 5. The vertical dashed line represents match points in the two photos.

The resistance of the dark coloration to a variety of cleaning methods suggested that it was an adherent oxide. The persistence of the dark oxide, position of the crack at the centerline of the outer weld deposit, and visible columnar texture of the crack surface all were consistent with a hot crack, a condition known to occur in submerged arc welds.

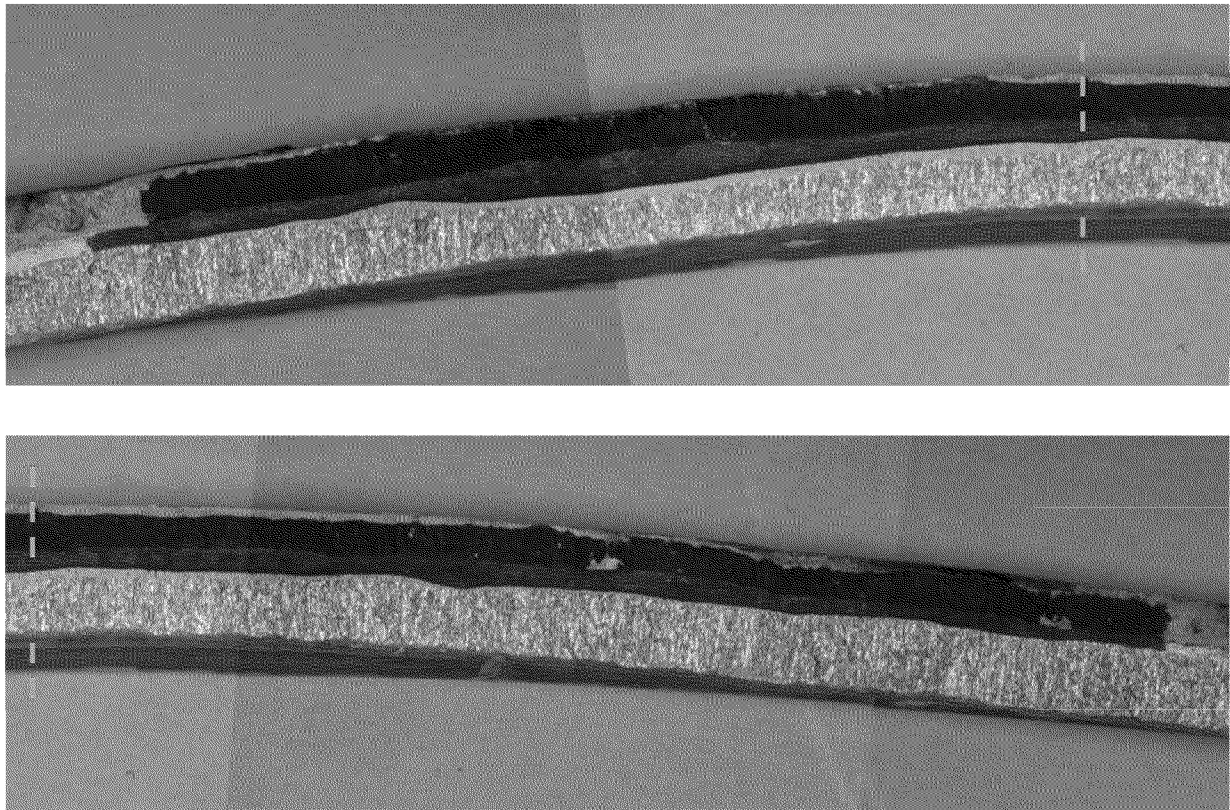


Figure 5. Composite of Origin, North Fracture Surface, After Cleaning, 2X (photo courtesy Exponent)

Microscopic Examination

The fracture was examined in a stereomicroscope to resolve features of interest, both before and after cleaning. Figure 6 shows a region of the fracture surface before cleaning. A dark, shiny deposit is evident near the exterior surface and on portions of the fracture in the outer weld deposit.

Figure 7 shows both ends of the defect, before cleaning. The dark coloration is present on the weld crack. The unfused surface is the flat region between the oxidized and nonoxidized weld fractures. The dark coloration on the LOP surface disappears beyond the portion that is coincident with the weld crack. The radial dimension of the LOP varied from 0.04 inch to 0.10 inch, based on viewing the surface under low magnification.

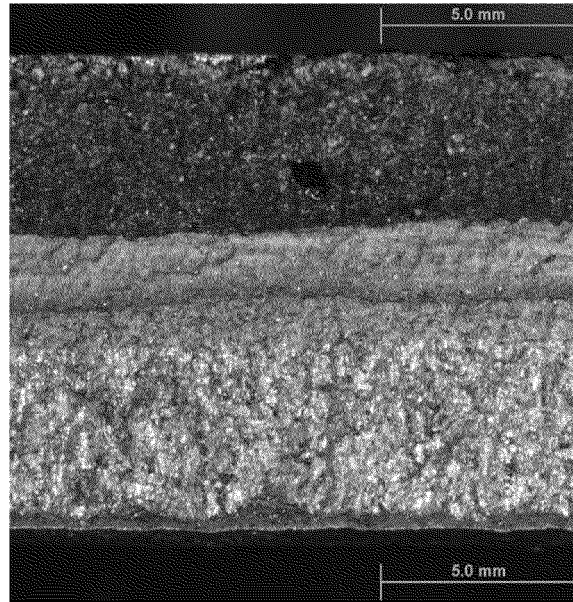


Figure 6. Fracture Surface Before Cleaning, 5X (photo by Exponent)

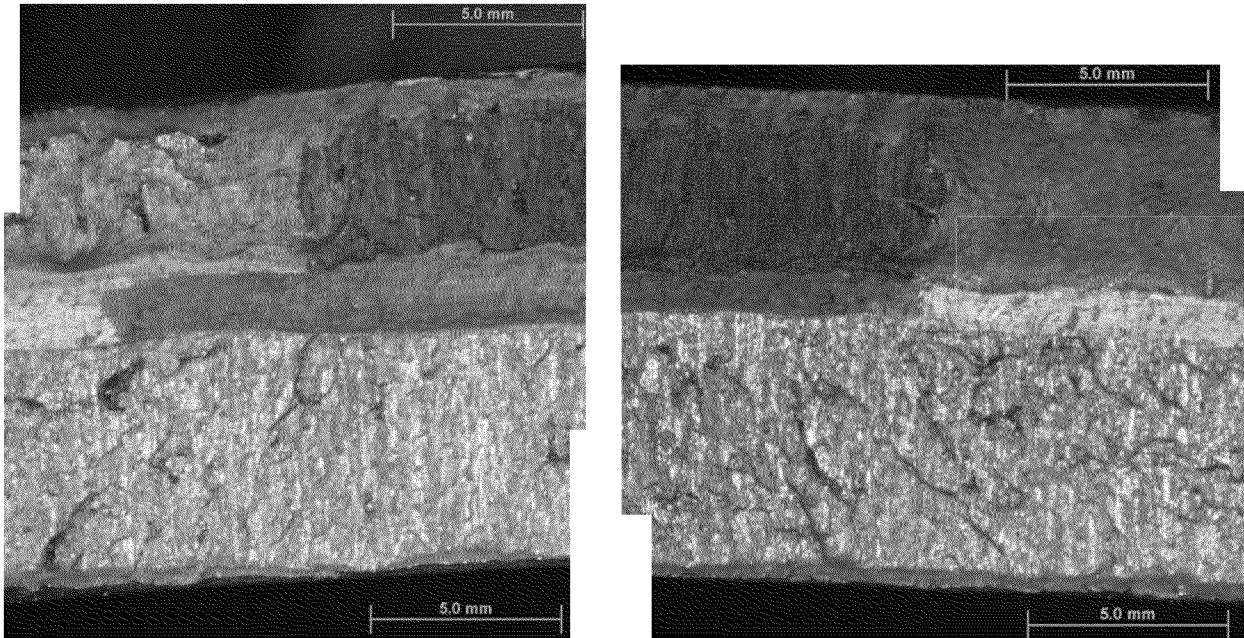


Figure 7. Terminations of Origin Defect, North Fracture Surface, 5X (photo by Exponent)

Photographs similar to those in Figure 6 and Figure 7 spanning the full length of the apparent origin and beyond were used to develop a profile of the radial dimensions of the apparent hot crack, the lack of fusion between the inner and outer weld beads, and the net thickness through the fracture plane. The profiles are given in Figure 8, as measured from the intersection of the fracture with the outside surface of the outer weld bead represented at the top of the chart. The average metal thickness through the fracture was 0.473 inch.

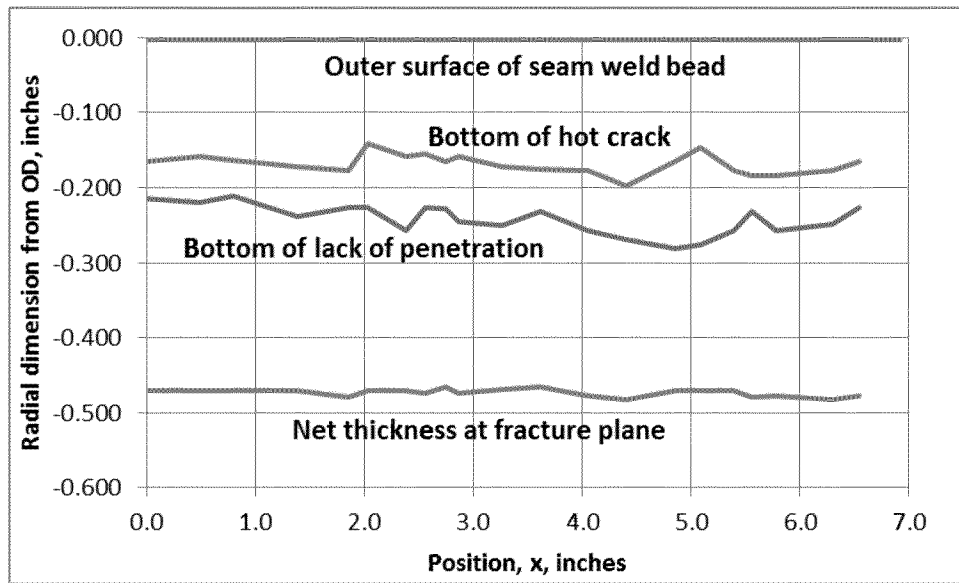


Figure 8. Radial Dimensions of Fracture Features

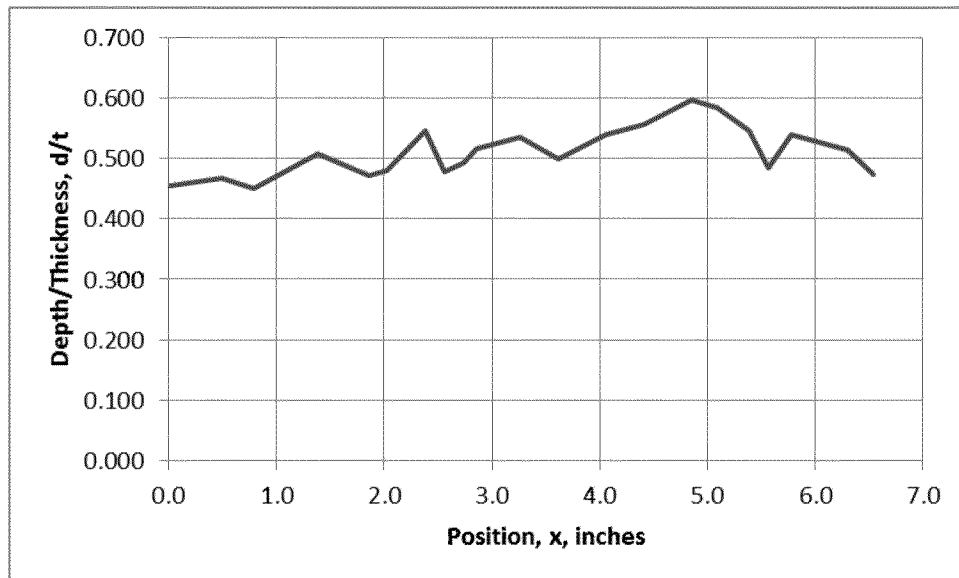


Figure 9. Ratio of Flaw Depth to Metal Thickness

The actual profile of the combined hot crack and LOP defect, from Figure 8, has a ratio of flaw depth to metal thickness (d/t) shown in Figure 9. The average d/t was 0.51 (51% of the metal thickness) with a maximum d/t of 0.60.

Scanning Electron Microscope Examination

A sample of the fracture surface was examined by scanning electron microscope (SEM) to resolve modes of fracture. Two examination sessions occurred, one in November attended by the author and a second session in January, not attended by the author. Selected photos from both sessions are presented. The SEM examination determined that there were six distinct fracture zones, positioned in the following order moving from the exterior surface to the interior surface, listed in Table 1.

Table 1. Fracture Zones Identified by SEM

Zone	Location	Description
1	Narrow zone between weld crack and exterior surface	Ductile
2	Weld crack in outer weld deposit	Oxidized, stained
3	Lack of penetration between inner and outer weld passes	Unfused, stained
4	Narrow zone below lack of penetration	Ductile
5	Primary fracture in inner weld deposit	Brittle
6	Narrow zone adjacent to interior surface	Ductile

These features are presented in a series of SEM images traversing from the outside surface to the inside surface. They are discussed following the photos.

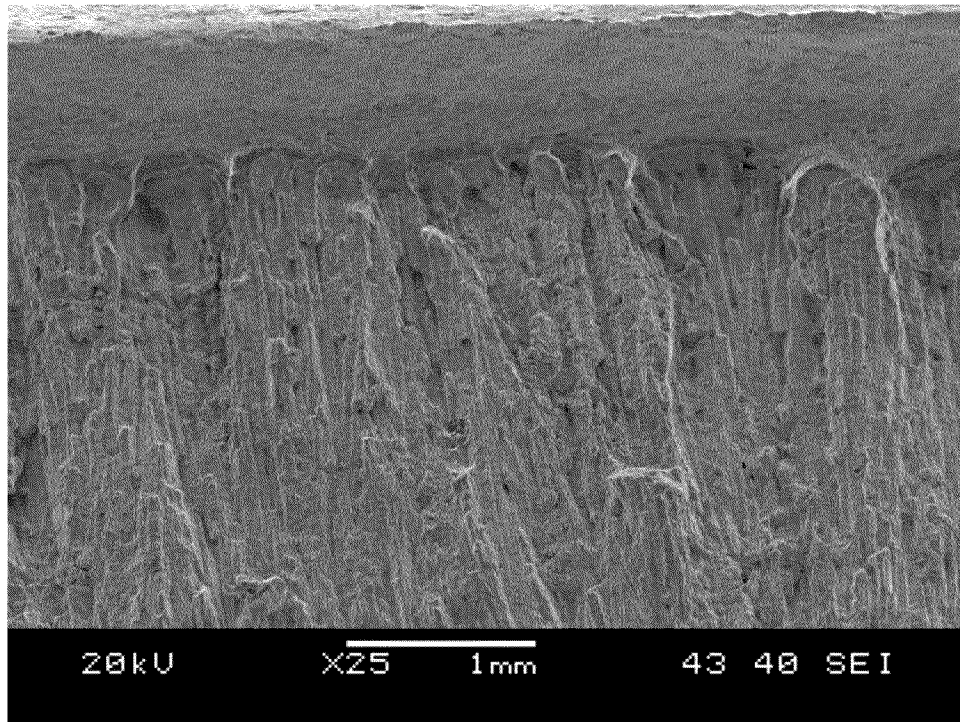


Figure 10. Zone 1 and Upper Part of Zone 2, 25X

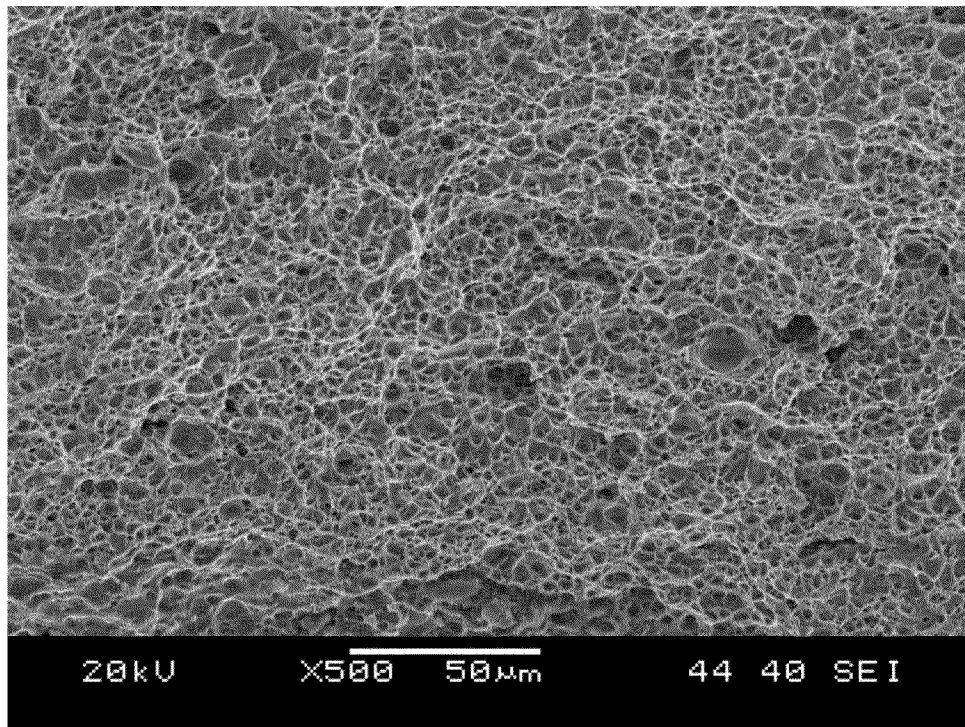


Figure 11. Detail in Zone 1, 500X

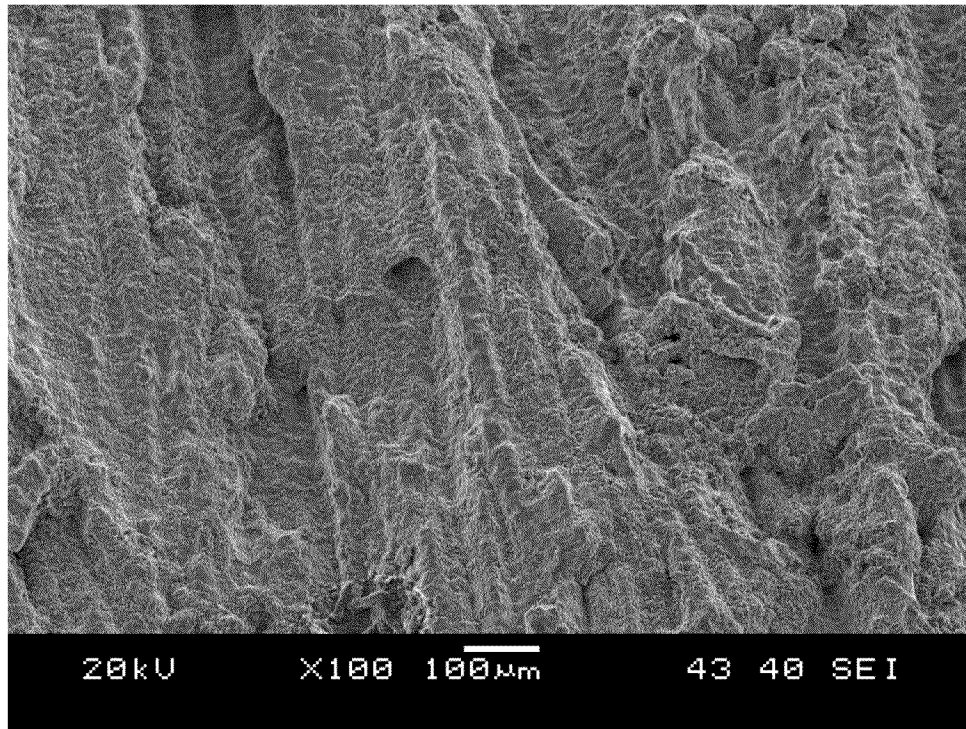


Figure 12. Zone 2 Surface, 100X

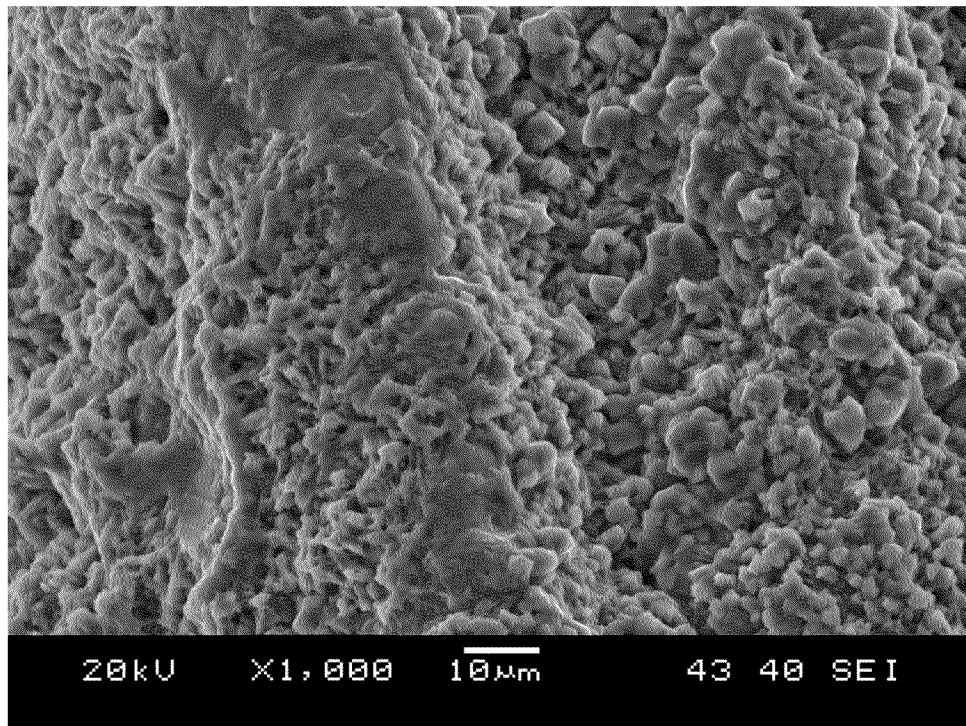


Figure 13. Detail of Zone 2, 1,000X

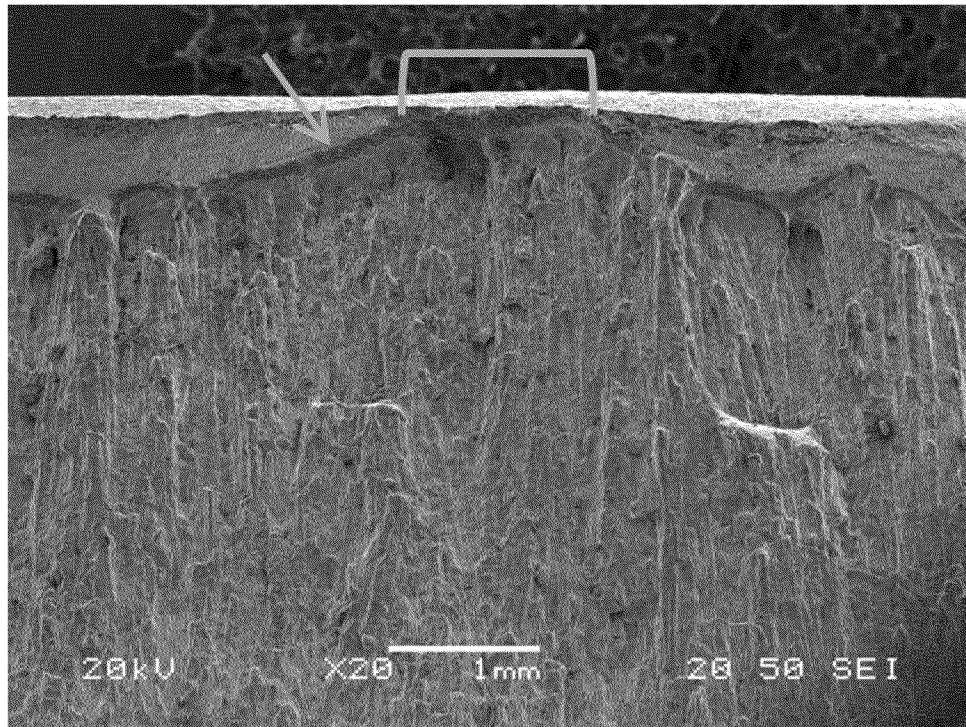


Figure 14. Local Extension of Zone 2 to Exterior Surface, 20X

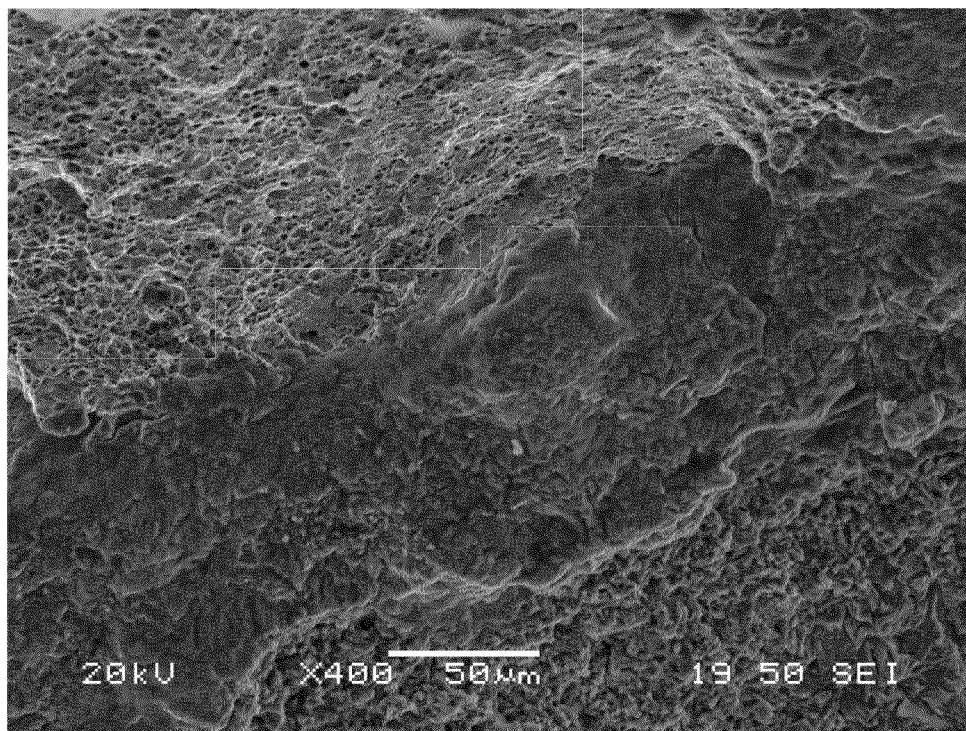


Figure 15. Detail at Edge of Zone 1 Extension, 400X

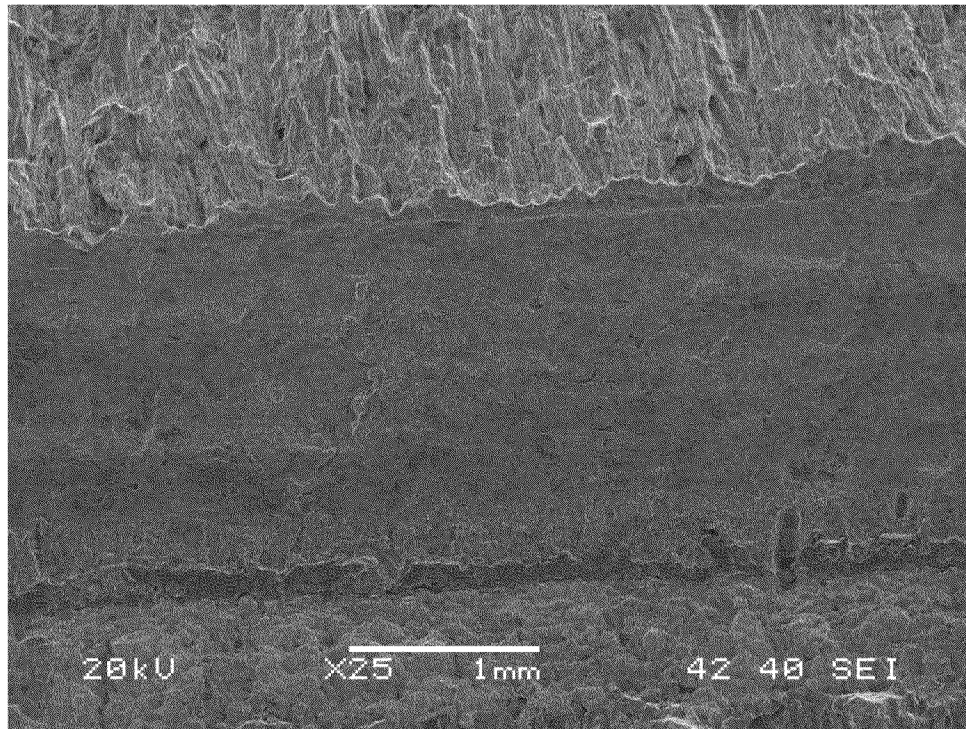


Figure 16. Zone 3 Surface, 25X

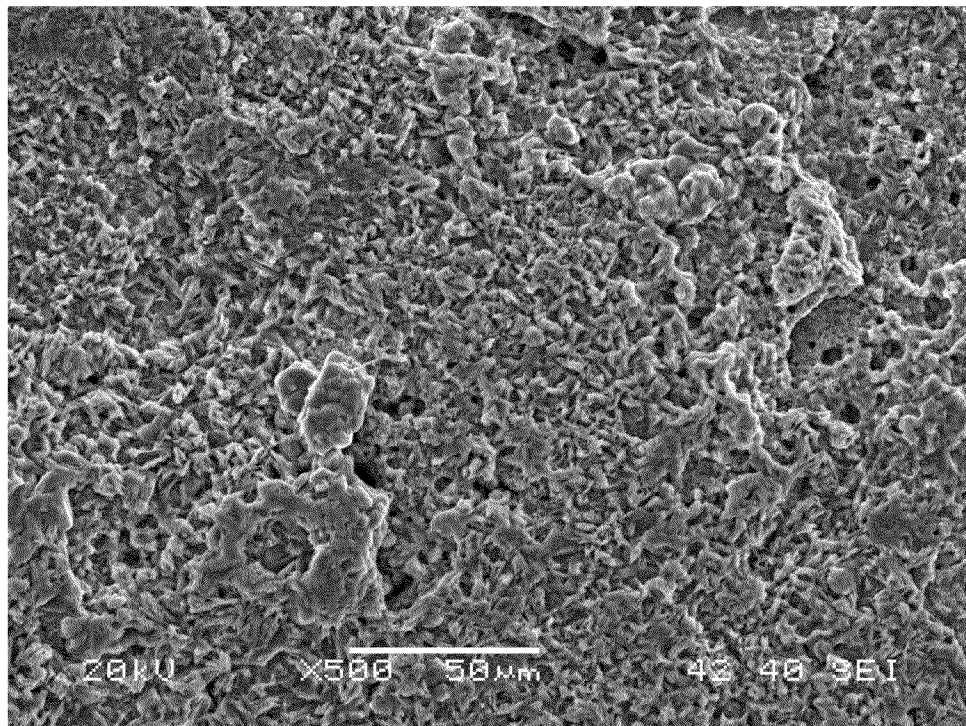


Figure 17. Detail of Zone 3, 500X

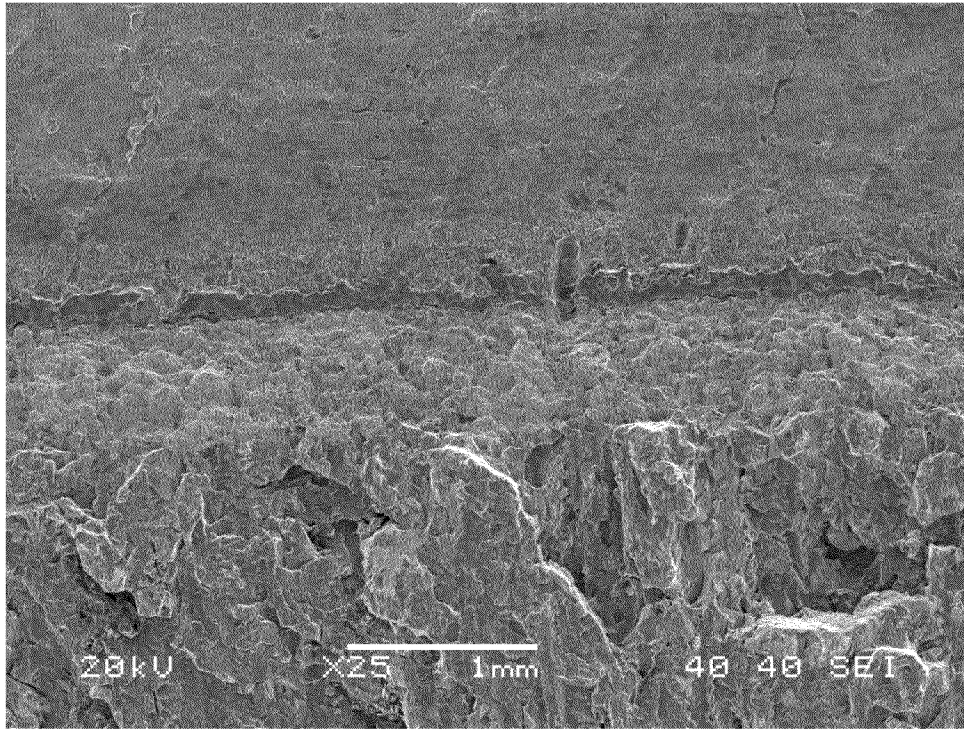


Figure 18. Zone 4 between Lower Part of Zone 3 and Upper Part of Zone 5, 25X

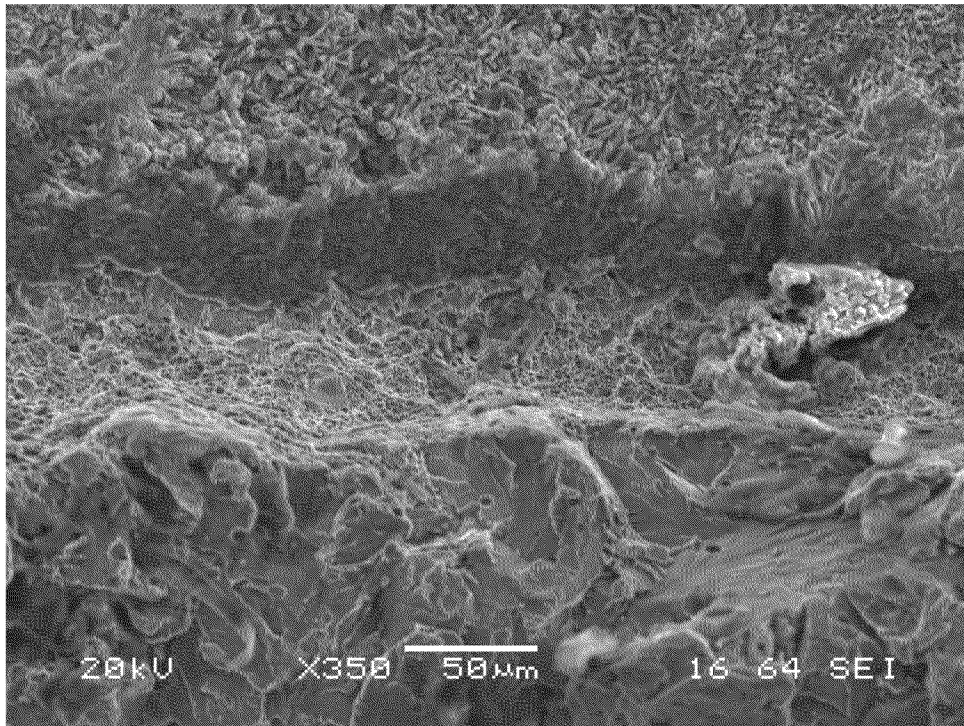


Figure 19. Detail of Zone 4, 350X

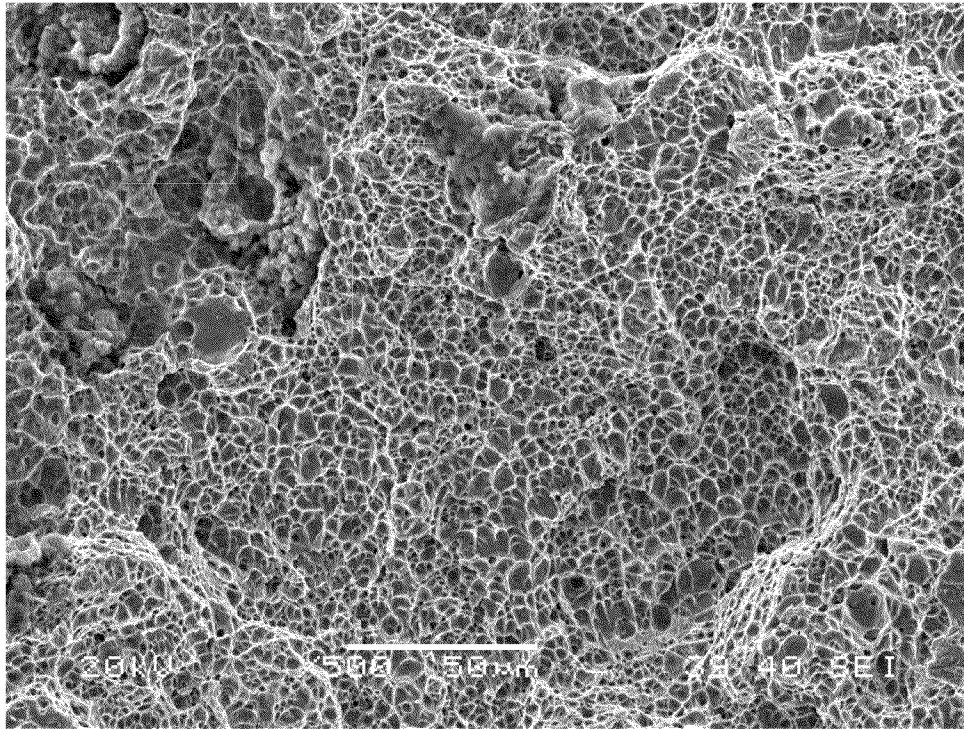


Figure 20. Detail of Zone 4, 500X

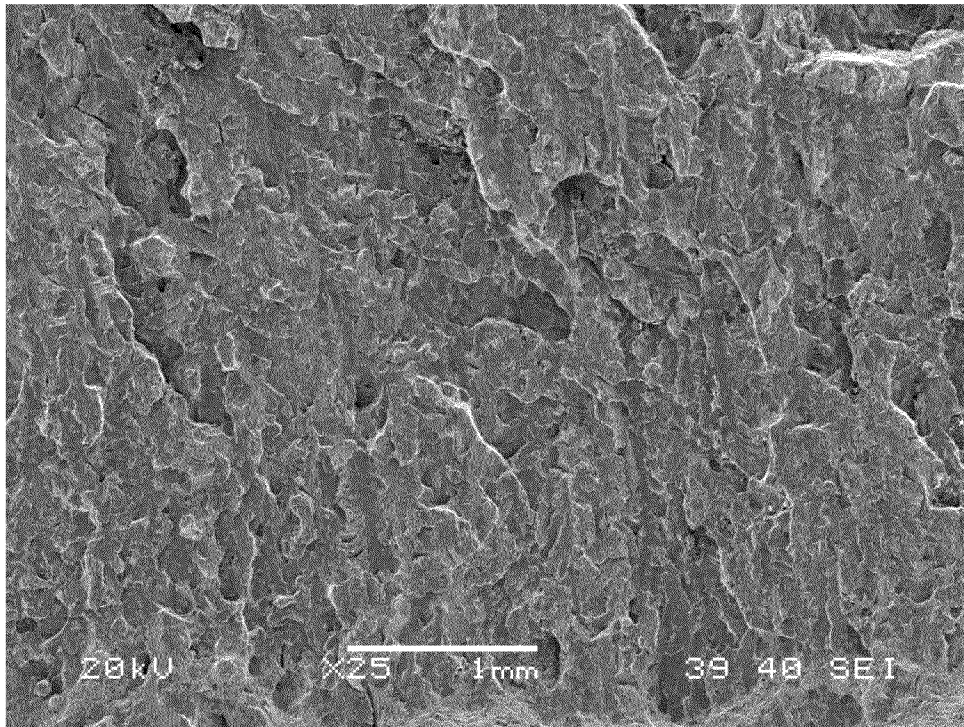


Figure 21. Zone 5 Surface, 25X

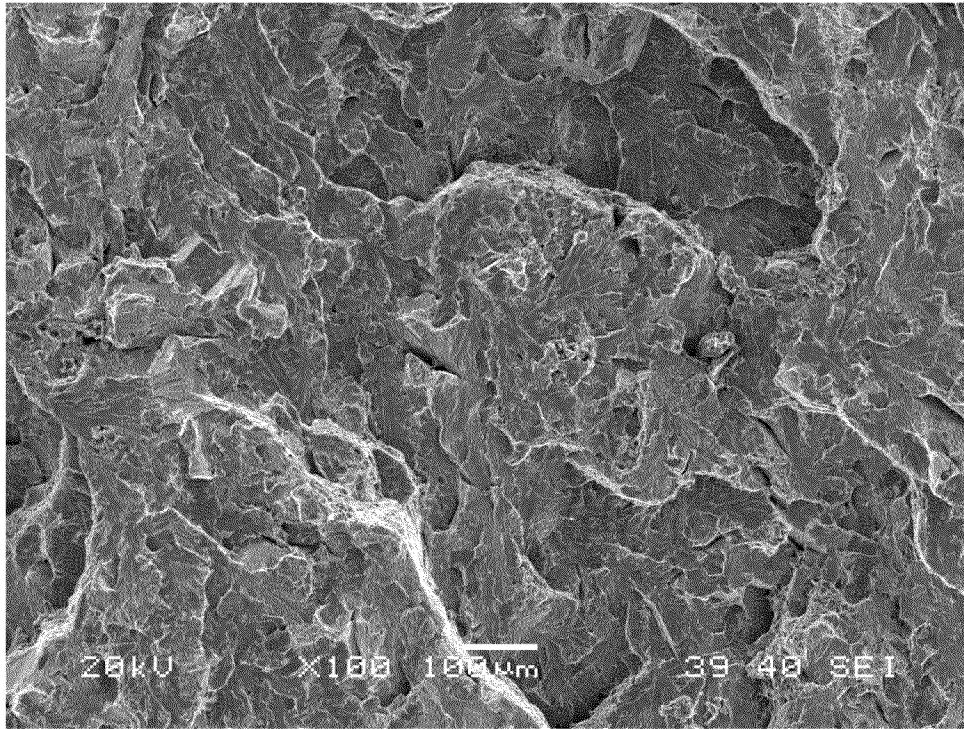


Figure 22. Detail of Zone 5, 100X

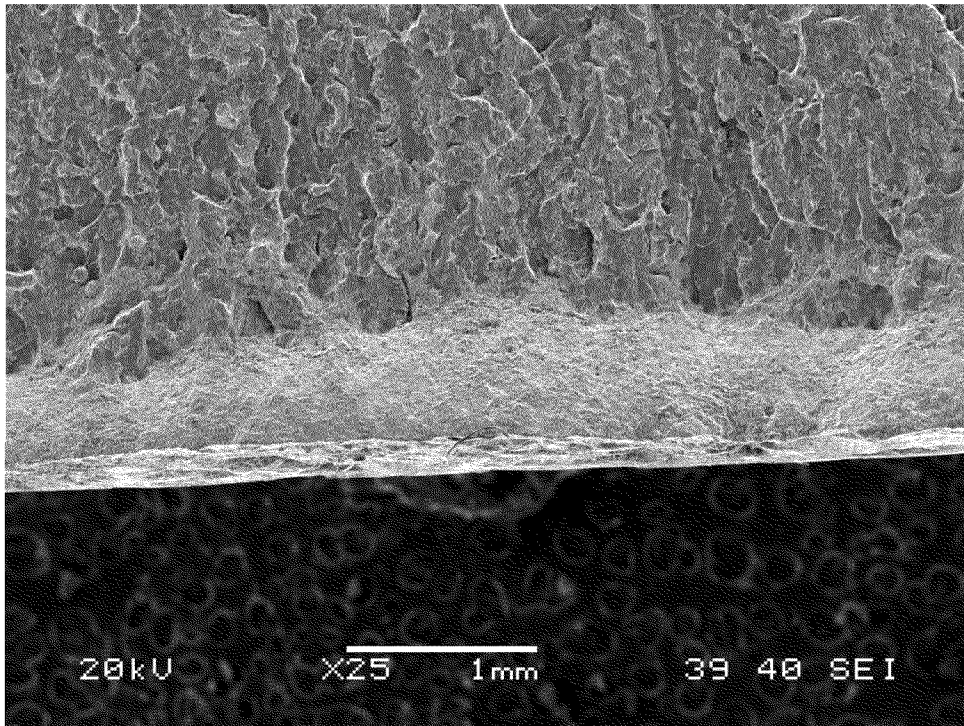


Figure 23. Zone 6 at Bottom of Zone 5, 25X

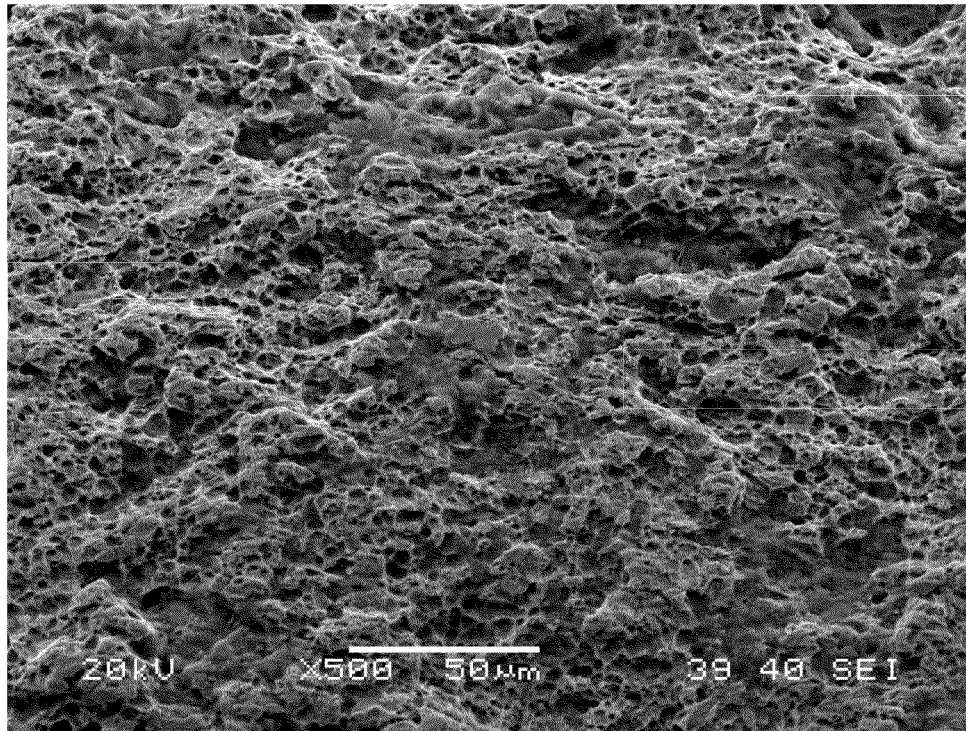


Figure 24. Detail of Zone 6, 500X

Figure 10 shows Zone 1 and the upper portion of Zone 2. Figure 11 is a detail of Zone 1 at high magnification exhibiting a dimpled texture indicating ductile fracture. Zone 1 is interpreted as a ductile shear lip that failed at the time of the hydrostatic test.

Figure 12 shows the typical surface in Zone 2. Zone 2 in Figure 12 and in the lower portion of Figure 10 exhibits the columnar structure of the apparent hot crack in the weld. Figure 13 is a detail of Zone 2 at high magnification. The surface is coated with an adherent oxide. Figure 14 shows a region where Zone 2 penetrates through Zone 1 to the pipe exterior surface (at bracket). The arrow identifies what appears to be extension of the flaw. Figure 15 is a detail of the extension feature at high magnification with Zone 1 in the upper left and Zone 2 in the lower right. While the feature between the two zones lacks the columnar structure of Zone 2, it is coated with an adherent oxide like Zone 2 suggesting that it experienced a similar environmental history as Zone 2. The identified region is interpreted as extension of the hot crack that occurred while the material was still hot.

Figure 16 shows the unfused surface comprising Zone 3 and representing the lack-of-penetration between the inner and outer weld beads. Zone 2 is in the upper part of the photo and Zone 4 is in the lower part. Figure 17 is a detail of Zone 3 at high magnification. The surface is covered with an adherent oxide.

Figure 18 shows a region of fracture comprising Zone 4. Zone 3 is in the upper part of the photo and Zone 5 is in the lower part. Figure 19 and Figure 20 are details in Zone 4 at intermediate and high magnification, respectively. Figure 19 and Figure 20 were not obtained at the same locations. The width of Zone 4 varied significantly. Zone 4 exhibited dimpled, ductile fracture with no oxide. Zone 4 is interpreted as the ductile initiation of the failure that occurred during the hydrostatic pressure test.

Figure 21 shows the typical surface in Zone 5. Figure 22 is a detail of Zone 5 at high magnification. The surface exhibits cleavage planes indicating brittle fracture, and no oxide. Zone 5 represents the propagation of the hydrostatic test fracture through the inner weld deposit.

Figure 23 shows Zone 6 adjacent to the interior pipe surface, and the lower part of Zone 5. Figure 24 is a detail of Zone 6 at high magnification, exhibiting dimpled, ductile fracture with some surface deposits. Zone 6 is interpreted to be a ductile shear lip that developed as the propagating fracture reached the interior surface.

Metallographic Sections

Metallographic sections were prepared through two positions in the 7-inch long apparent hot crack. Composite photographs of metallographic sections through two positions in the origin defect are presented in Figure 25 and Figure 26. Mount "A" was obtained from the upstream end of the hot crack and Mount "B" was removed from the downstream end. The photos are oriented with the pipe exterior surface as the upper surface. The apparent hot crack, LOP, and hydrostatic test fracture are identified.

The inside and outside weld deposits are seen to penetrate to a depth of approximately half of the pipe wall thickness. Penetration was intended to be $2/3$ of the wall thickness in order to provide overlap.¹ Also, the outer weld deposit is seen to be offset laterally approximately 0.2 inch, causing the deepest points of penetration of the two weld passes to miss each other.

¹ Moody Engineering Company, Inspection of Consolidated Western Pipe Order 7R-66858 for 30" O.D. x 3/8" Gas Pipe, Letter report to PG&E, July 19, 1949.

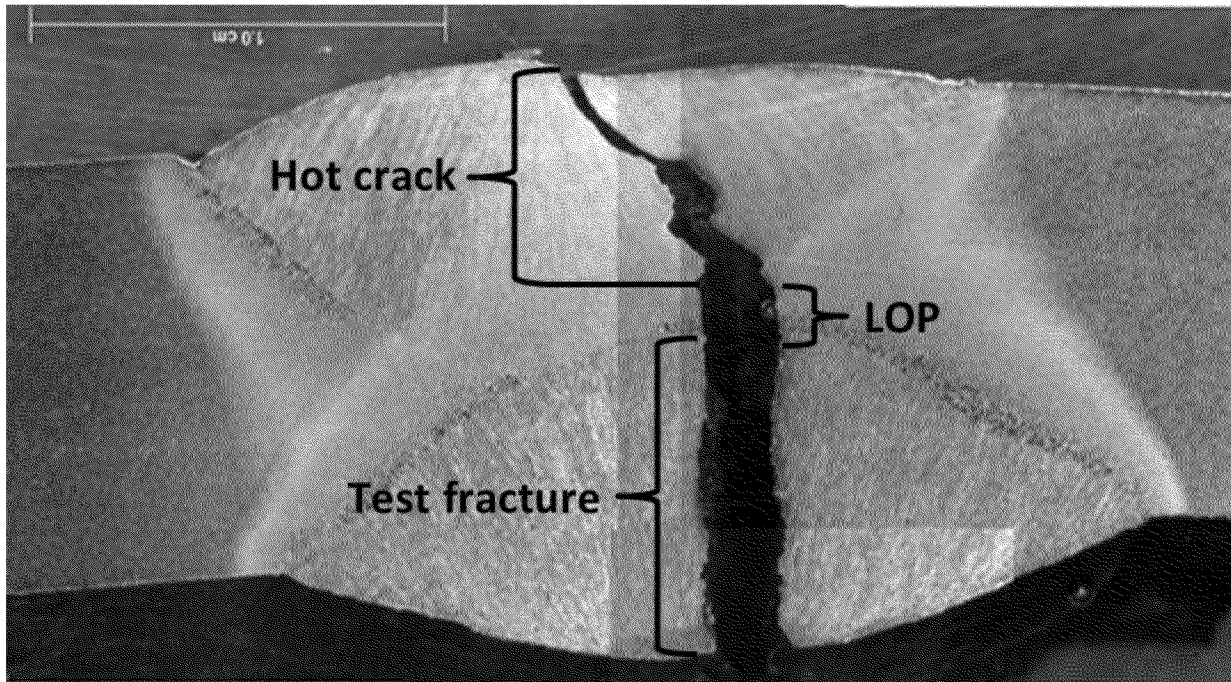


Figure 25. Metallographic Cross Section, Mount A, 5X

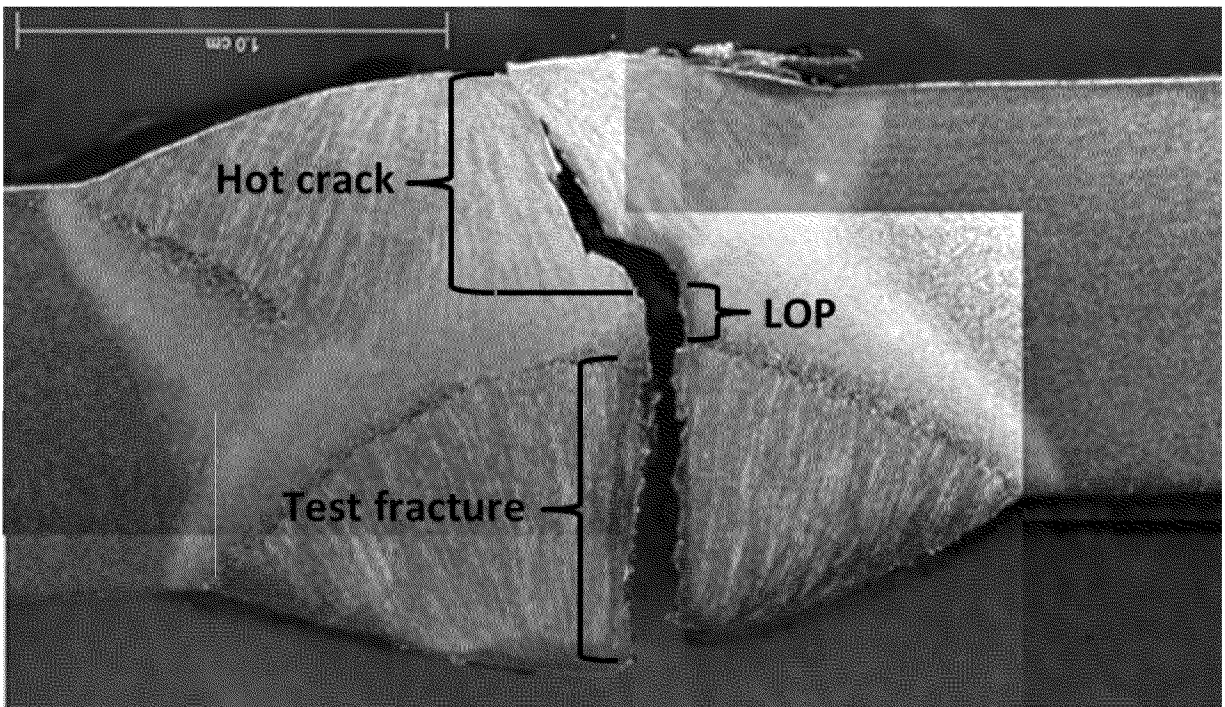


Figure 26. Metallographic Cross Section, Mount B, 5X

Metallographic sections were also prepared through unfractured portions of the longitudinal seam, one of which (from piece 72493) is shown in Figure 27. The section shows that the outside pass was made first because the inside weld deposit is seen to overlap the outside weld

deposit. There is no LOP feature even with some lateral misalignment of the weld deposits because overlapping penetration was achieved.

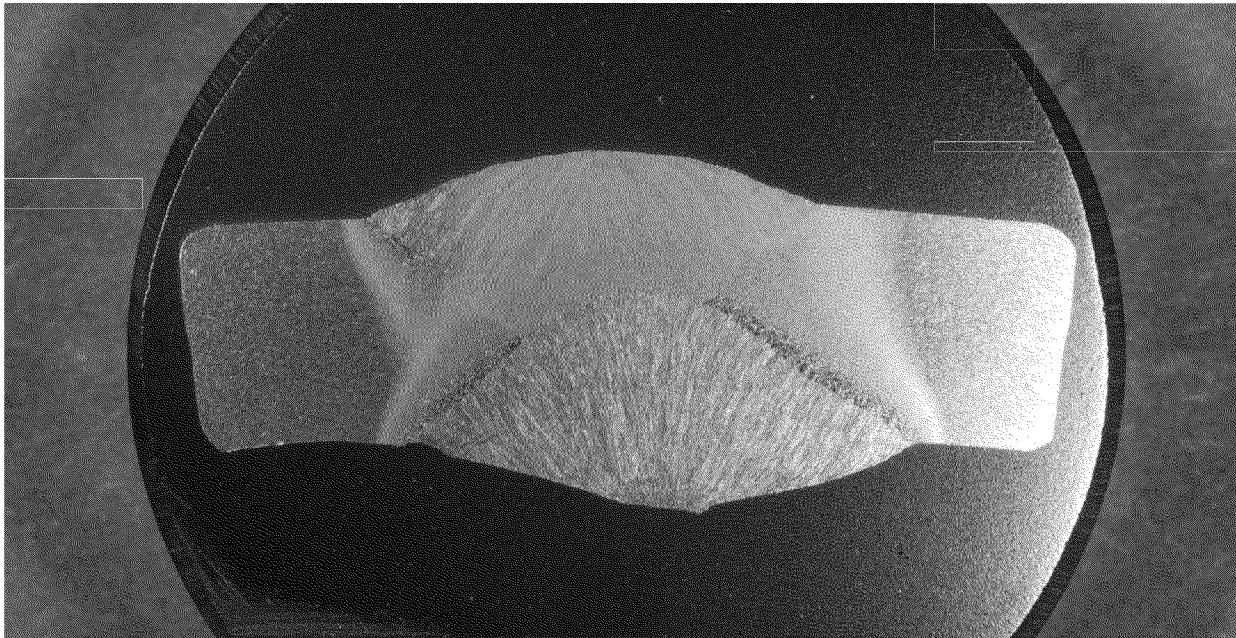


Figure 27. Intact Seam Showing Normal Seam Weld Deposition

Other metallographic sections were prepared through the longitudinal seam and a surface imperfection in the plate identified by nondestructive examination. These are presented in Appendix A. A section in the seam confirmed another apparent hot crack in the outer seam weld deposit having a radial dimension of approximately 0.12 inch. It was small and uninvolved in the test break.

Material Properties

Several coupons were removed from the failed pipe for testing of material properties. The testing was performed by Anamet, Inc., Hayward, CA under the direction of PG&E.

Tensile Tests

Tensile tests were performed on two plate samples and two seam weld samples, in accordance with API 5L and ASTM A370. The tensile test specimens were flattened transverse straps. The yield strength was established at 0.5% extension under load and elongation was measured over a 2-inch gage length. The results are summarized in Table 2.

Table 2. Tensile Testing Results

Sample	Material	Yield, ksi	Tensile, ksi	Elong., %	Fracture Location
T-117-CE-LS-WE-1	Seam	73.9	90.2	20	Base metal
T-117-CW-LS	Seam	76.8	91.6	12.7	Weld
T-117-1-E-LS	Seam	69.3	88.8	20.5	Base metal
T-117-2-W-LS	Seam	71.6	89.0	18.5	Base metal
T-117-CE-LS-W-B	Plate	65.5	85.4	31	n/a
T-117-CW-B	Plate	67.7	86.5	31	n/a
T-117-1-E-BM	Plate	67.8	85.6	30.5	n/a
T-117-2-W-BM	Plate	66.0	88.3	29.5	n/a

API 5LX, 2nd Edition, which was in effect in 1949 when this pipe was manufactured, only specified properties for Grade X42 line pipe.² At that time, API 5LX allowed the manufacture of higher-strength grades in accordance with the manufacturing, inspection, and testing methods, with properties by agreement between manufacturer and purchaser. Strength properties for Grade X52 were not specified by API 5LX until the 4th Edition in 1953. Thus the manufacture of this pipe was in accordance with specifications agreed between Consolidated Western and PG&E. PG&E's purchase specification for 34-inch OD pipe with 11/32-inch wall thickness at that time specified minimum yield strength of 52 ksi, minimum tensile strength of 72 ksi, and minimum elongation of 22%.³ These same minimum specified properties were also stated in a PG&E specification for 34-inch OD pipe with 3/8-inch wall thickness and thinner to be manufactured by Consolidated Western in 1953.⁴ The seam was required to exhibit a tensile strength at least equal to the specified minimum tensile strength of the plate. Yield and elongation properties were not specified. The test results met the specified strength properties.

CVN Impact Tests

Charpy V-Notch (CVN) impact tests were performed on four plate samples and four weld metal samples. The samples tested and the test temperatures are listed in Table 3. CVN specimens were 8-mm x 10-mm x 55 mm, oriented transversely and with the notch machined in the through-thickness direction so as to fracture in the test in the same direction with respect to the material as an axially propagating fracture.

² Specification for High-Test Line Pipe, Specification 5LX, American Petroleum Institute, May 1949.

³ Specification for 34" O.D. Gas Line Pipe for Pacific Gas & Electric Company, PGE-7, September 16, 1948.

⁴ Specification for 34" O.D. Gas Line Pipe for Pacific Gas & Electric Company, Revised 1-8-53.

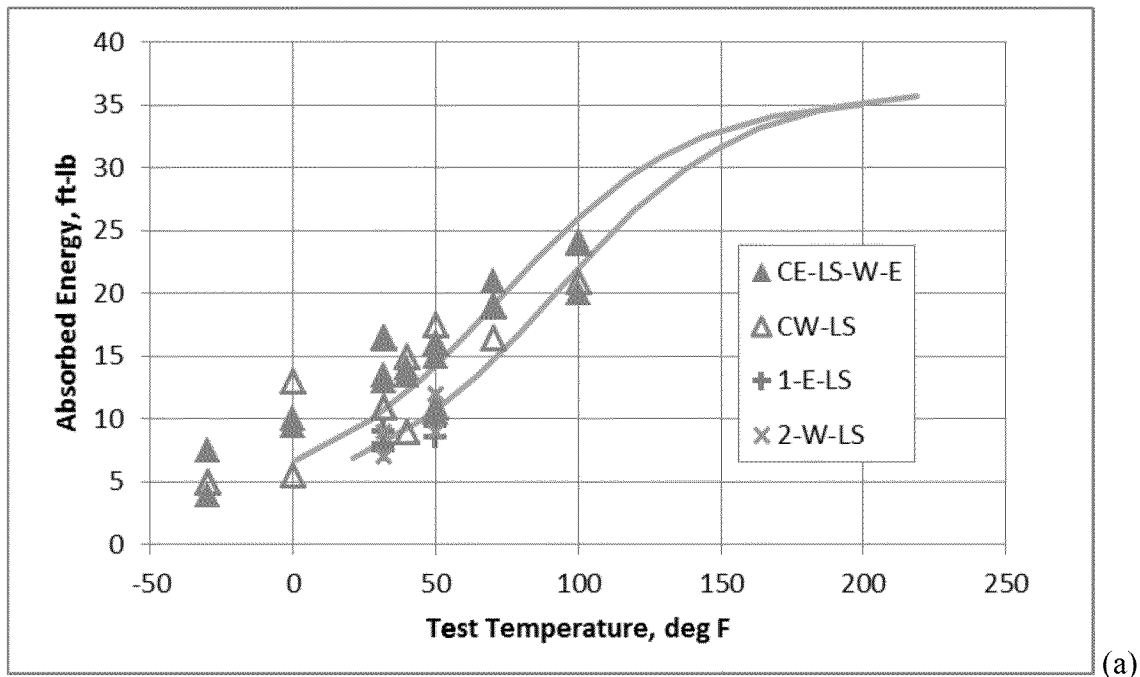
Table 3. CVN Specimen Test Temperatures

Specimen	Material	Test Temperatures, F (No. of Tests)
T-117-CE-LS-W-E	Seam weld	-30 (2), 0 (2), 32 (3), 40 (2), 50 (3), 70 (2), 100 (2)
T-117-CW-LS	Seam weld	-30 (2), 0 (2), 32 (3), 40 (2), 50 (3), 70 (2), 100 (2)
T-117-1-E-LS	Seam weld	+32 (3), +50 (3)
T-117-2-W-LS	Seam weld	+32 (3), +50 (3)
T-117-LS-W-B	Base metal	-30 (2), 0 (2), 32 (3), 40 (2), 50 (3), 70 (2), 100 (2)
T-117-CW-B	Base metal	-30 (2), 0 (2), 32 (3), 40 (2), 50 (3), 70 (2), 100 (2)
T-117-1-E-BM	Base metal	+32 (3), +50 (3)
T-117-2-W-BM	Base metal	+32 (3), +50 (3)

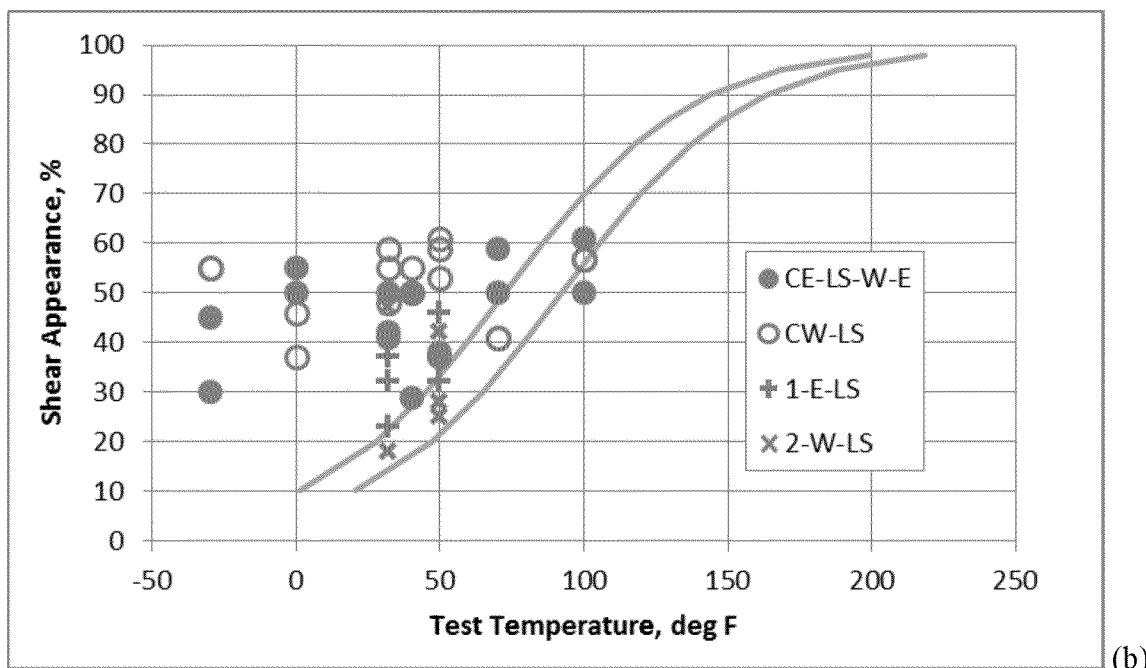
The absorbed impact energy and shear appearance are shown in Figures 28(a) and 28(b) for the seam weld specimens, and in Figures 29(a) and 29(b) for the pipe body specimens. The weld shear appearance results exhibited more scatter than the plate specimens.

The tests were not performed to a sufficiently high temperature to capture the full toughness transition curve up to the ductile upper shelf or 100% shear appearance. For purposes of interpretation, the full transition curves were extrapolated using an empirical technique.⁵ The extrapolated curves were prepared using the averaged test results at the two warmest test temperatures, 70 F and 100 F. Extrapolations from these two temperatures were fairly consistent.

⁵ Rosenfeld, M.J., "A Simple Procedure for Synthesizing Charpy Impact Energy Transition Curves from Limited Test Data", ASME First International Pipeline Conference, Calgary, 1996.



(a)



(b)

Figure 28. CVN Test Results for Seam Weld Specimens

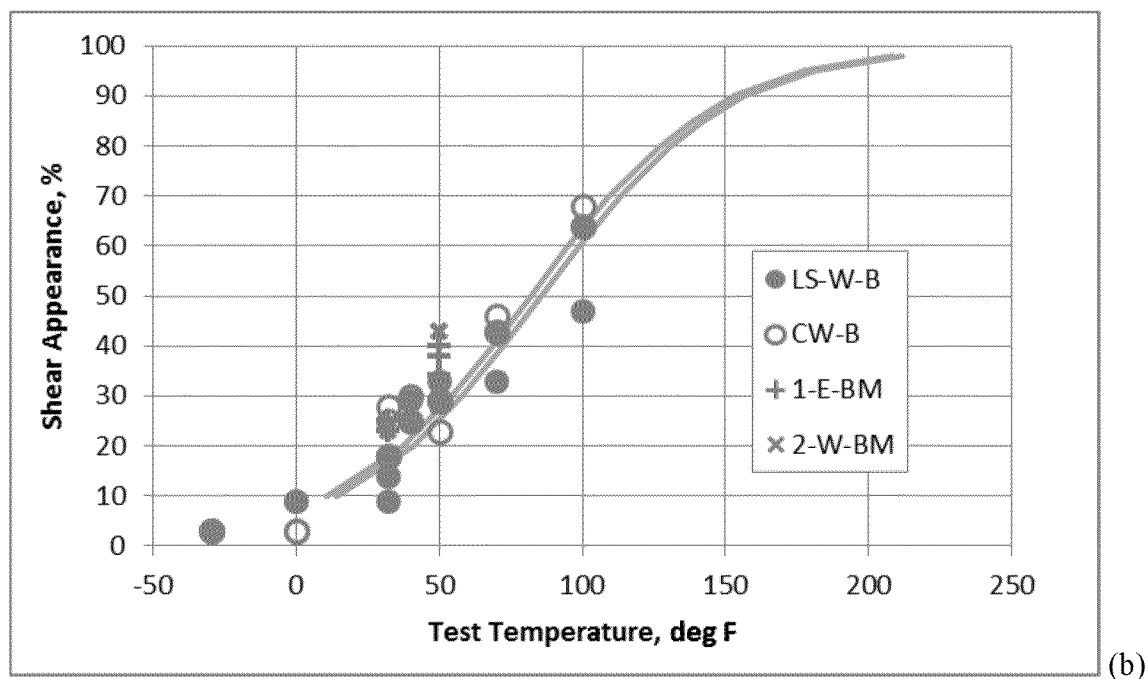
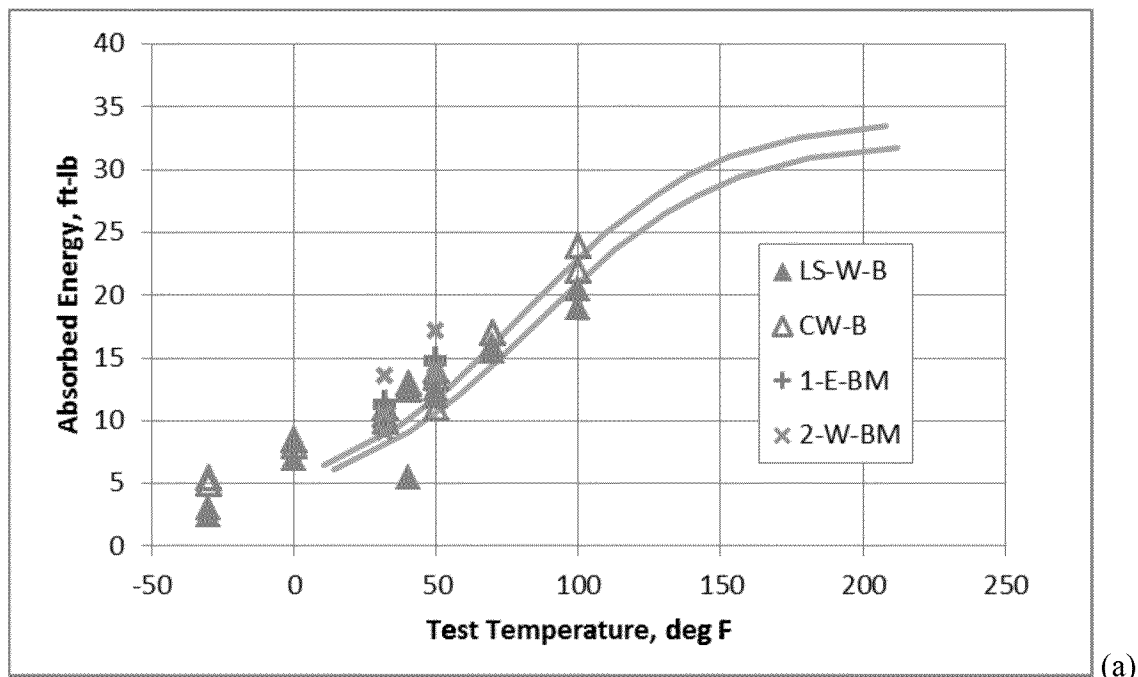


Figure 29. CVN Test Results for Pipe Body Specimens

The interpreted CVN properties are summarized in Table 4. The upper shelf absorbed energy for the 80% full-size CVN specimens was estimated to be 35 ft-lb for the weld and 33 ft-lb for the pipe body, corresponding to equivalent full-size (10-mm x 10-mm specimen) upper shelf absorbed energy levels of 44 ft-lb and 41 ft-lb, respectively. The 80% full-size CVN specimens are 2/3 of the full-scale thickness of the plate and weld so no adjustment for a specimen-size

effect is necessary to interpret the transition temperature.⁶ The results indicate that the transition temperature defined by 50% Shear Appearance, and the minimum upper shelf temperature defined at 85% Shear Appearance are both well above the typical operating temperature. This is consistent with the brittle fracture observed on the test fracture surfaces even though the upper shelf absorbed energy exceeds the arrest toughness of 34 ft-lb.⁷ Fracture control was not a recognized practice in the design of gas pipelines, and CVN properties were not specified by API 5LX or PG&E specifications, at the time this pipe was manufactured.

Table 4. Interpreted CVN Test Results

Material	Full-size Equiv. Upper Shelf, ft-lb	Transition Temperature at 50% SA, deg F	Upper Shelf Temperature at 85% SA, deg F
Seam weld	44	72-92	129-149
Pipe body	41	82-85	141-148

Material Chemistry

The chemistry of four samples of base metal was determined and the results are listed in Table 4 by weight percent. The chemistry requirements for Grade X52 were not specified in API 5LX until the 1954 5th Edition. The chemistry results conformed to the requirements of the 1948 and 1953 PG&E specifications for large-diameter X52 line pipe cited previously. The chemistry was typical for line pipe of the designated type and era of manufacture. The chemistry of the deposited seam weld metal was not tested.

The Carbon Equivalent (CE) is an empirical measure of weldability. For steels with C>0.12%, CE is calculated using the IIW formula.⁸ CE levels in excess of 0.43% correlate to increased susceptibility to hydrogen assisted cracking associated with welding under high cooling rate conditions.

Susceptibility to hot cracking in submerged arc welding of carbon steel can be related to the chemistry of the base metal in accordance with the “units of cracking susceptibility” (UCS). UCS values above 30 indicate a low resistance to hot cracking.⁹ The base metal chemistry is an indicator because submerged arc welds consist of significant amounts (30% to 70%) of remelted base metal, however, other factors such as restraint and weld bead profile also affect susceptibility to hot cracking.

⁶ Ibid., Rosenfeld.

⁷ B31 Code for Pressure Piping, Section 8, “Gas Transmission and Distribution Piping Systems”, B31.8, ASME, 2010.

⁸ Lancaster, J.F., *Metallurgy of Welding*, Sixth Edition, Abington Publishing, 1999.

⁹ BS EN 1011-2: 2001, “Welding - Recommendations for welding of metallic materials - Part 2: Arc welding of ferritic steels”, BSI and CEN.

Table 5. Material Chemistry Data

Element	T-117-CE-LS-W-B	T-117-CW-B	T-117-1-E-BM	T-117-1-E-BM	PGE-6 ^(a)
Carbon (C)	0.28	0.27	0.29	0.30	0.30+0.04
Chromium (Cr)	0.02	0.03	0.01	0.03	--
Columbium (Cb)	<0.005	<0.005	<0.005	<0.005	--
Copper (Cu)	0.07	0.04	0.08	0.09	--
Manganese (Mn)	0.95	0.93	1.02	1.03	1.2 +0.04
Molybdenum (Mo)	<0.005	<0.005	<0.005	<0.005	--
Nickel (Ni)	0.06	0.07	0.08	0.08	--
Phosphorus (P)	0.011	0.023	0.012	0.023	0.045+0.01
Silicon (Si)	0.05	0.07	0.07	0.06	--
Sulfur (S)	0.027	0.025	0.055	0.040	0.05+0.01
Titanium (Ti)	<0.005	<0.005	<0.005	<0.005	--
Vanadium (V)	<0.005	<0.005	<0.005	<0.005	--
CE _{IW} ^(b)	0.453	0.440	0.475	0.491	--
UCS ^(c)	63.8	61.9	70.9	71.3	--

(a) Ladle maximum allowed + check analysis maximum variance

(b) Carbon Equivalent, $CE_{IW} = C + Mn/6 + (Cr+Mo+V)/5 + (Cu+Ni)/15$

(c) Units of Cracking Susceptibility, $UCS=230C + 190S + 75P + 45Nb - 12.3Si - 5.4Mn - 1$

DISCUSSION

The Hot Crack

The failure originated at a hot crack embedded in the outside pass of the double submerged-arc weld (DSAW) longitudinal seam. The outside pass was deposited before the inside weld pass. The hot crack was 6.5 inches long and extended radially through most of the outer weld deposit.

Hot cracking occurs as the deposited weld solidifies. Solidification reduces the solubility of impurities or alloying elements and drives them toward the core of the weld deposit which is the last portion of the weld to freeze. The impurities become trapped at grain boundaries in the weld interior where they lower the melting point. The weld shrinkage stresses cause the still-liquid or mushy grain boundaries to separate.

The reason for the formation of this particular hot crack is unknown, but the occurrence of hot cracks in line pipe seams manufactured using the submerged-arc welding process is not unknown. Influences on hot cracking include base metal chemistry, weld bead profile, and applied stress on the solidifying weld. High carbon, sulfur, and phosphorus content in the base metal tend to increase susceptibility to hot cracking. The chemistry of the base metal exceeded an empirical threshold indicating low resistance to hot cracking, although the chemistry was typical for line pipe of the designated grade and era of manufacture. Single submerged arc weld

deposits that are deeper than they are wide are more prone to hot cracking. The weld deposit in the test failure was wider than it was deep so the bead geometry did not promote hot cracking. Historical inspections of pipe produced by Consolidated Western have indicated a tendency for hot cracking to occur at the pipe ends due to insufficient restraint of elastic springing of the pipe in their welding fixtures.¹⁰ Although this crack did not occur precisely at the pipe end, it was located within 1.5 ft of the end and could have been influenced by end restraint conditions. A less severe hot crack that remained intact and that was uninvolved in the test failure was identified in another metallographic section elsewhere in the seam.

The Lack of Penetration

The LOP condition extended upstream and downstream of the hot crack. Metallographic sections indicated that the LOP was due to lateral offset of the outer weld bead such that the points of maximum penetration of the inner and outer weld passes did not coincide. Bead offset is seen occasionally in DSAW seams of all vintages. The penetration was just enough for the inner and outer welds to touch if they were perfectly aligned. The offset and penetration enabled the abutting plate edges to remain unfused at mid-wall-thickness. The LOP condition would not have been detectable by visual inspection or by hydrostatic pressure testing to prescribed pressure test levels.

The unfused surfaces associated with the LOP exhibited a dark discoloration interpreted as a tempering effect reflecting the thickness of oxide film formed by exposure to air while at a high temperature. A black oxide corresponds to temperatures above 800 F. The zone immediately below the penetrated area of a submerged arc weld can remain above 800 F for as long as 30 seconds.¹¹ The LOP surfaces were likely exposed while still hot to air that entered where Zone 2 of the hot crack extended to the exterior surface over a 0.04-inch (1-mm) length.

Fracture Assessment

The hot crack was an original manufacturing defect which survived the hydrostatic pressure test conducted by the pipe manufacturer at the mill. The field test failure occurred at a higher pressure (998 psig) than the pipe mill test pressure (945 psig).

In order to understand the behavior of the flaw, the failure pressure was estimated using a recognized relationship between flaw size and failure stress level in a pressurized cylinder,¹²

¹⁰ Ibid, Moody Engineering.

¹¹ Linnert, G.E., *Welding Metallurgy, Volume 1*, American Welding Society, 4th Edition, 1995.

¹² Kiefner, J.F., "Modified Assessment Aids Integrity Management" (Part 1) and "Modified Ln-Secant Equation Improves Failure Prediction" (Conclusion), *Oil & Gas Journal*, Oct. 6 and Oct. 13, 2008.

modified to consider the actual profile of the defect.¹³ The analysis was performed using the flaw profile in Figures 8 and 9, along with the lowest measured seam yield strength and tensile strength values of 69 ksi and 89 ksi, respectively, and an average metal thickness of 0.473 inch in the portion that fractured. Considering the flaw to be strictly flow-stress dependent (which would be the case with a blunt metal-loss defect, or a planar flaw in a material having very high toughness), the estimated failure pressure was 1,556 psig. This estimate significantly exceeded the actual failure pressure of 998 psig, indicating a toughness-dependency and/or an interaction with the LOP extending beyond the hot crack.

Considering the flaw to be a toughness-dependent crack with extrapolated full-size-equivalent CVN upper-shelf of 44 ft-lb, the estimated failure pressure was 1,129 psig, which still exceeded the actual failure pressure. The full-size-equivalent CVN would have to be 33 ft-lb for the estimated failure pressure to coincide with the actual failure pressure of 998 psig.¹⁴ This toughness level is less than what was actually measured in the sub-size CVN specimens. The implication is that the extended LOP interacted with the hot crack to lower the failure pressure.

The effect of the LOP was accounted for by extending the hot crack with a surface flaw having a depth equal to the radial dimension of the LOP extending 14 inches to either side of the hot crack. Using the minimum measured weld metal strength and the extrapolated full-size CVN impact energy of 44 ft-lb produced an estimated failure pressure of 995 psig, which was almost identical to the actual failure pressure.

An analysis of the hot crack alone without the LOP predicted a failure pressure of 1,160 psig. An analysis of the LOP alone predicted a failure pressure of 1,070 psig. These results indicate that the neither the hot crack nor the LOP, acting individually or separately, would have failed in the hydrostatic test. The test failure was therefore a result of the two flaws occurring together.

The hot crack and LOP exhibited no evidence of enlargement in service, e.g. due to fatigue crack growth. The combined defect exhibited small amounts of ductile flaw growth under hydrostatic test conditions immediately prior to the test failure. Flaw growth is not believed to have occurred during the mill test because the failure was toughness-dependent and yet survived a longer duration at a higher pressure than the mill test.

¹³ KAPA.xls, www.kiefner.com

¹⁴ The failure stress level of a flaw in a pressurized cylinder has been shown to correlate with the upper shelf CVN absorbed impact energy, even when the material is below the CVN upper shelf. This occurs for the following reason. The initiation of the fracture event occurs under quasi-static conditions, until the fracture accelerates. The toughness transition temperature under quasi-static conditions is lower than the transition temperature under dynamic conditions (as measured by the CVN test) by anywhere from 60 F to as much as 200 F. As a result, ductile fracture initiation can occur at temperatures well below the lowest temperature of the CVN upper shelf. This failure exhibited as small amount of ductile fracture initiation before the fracture transitioned to brittle propagation.

APPENDIX A: OTHER IMPERFECTIONS ON SAMPLE PIPE

Several features or imperfections were discovered in the course of examining the subject pipe. These included repairs of the submerged arc welded seam, a small solidification crack in an intact portion of the seam, and a small imperfection in the pipe body. The presence of these features had no effect on the outcome of the hydrostatic test and did not impair the integrity of the pipe while it was in service. Photographic information is presented here in the interest of completeness.

Longitudinal Seam Repairs

Repairs of the longitudinal seam by welding were identified in two locations. Repair of longitudinal seams by welding has been and continues to be an accepted practice both in pipe manufacturing specifications (e.g. API 5L) and pipe purchase specifications. The repair involves removal of the indicated weld defect by mechanical chipping or arc gouging, and rewelding the affected portion using a suitable weld process which could include submerged arc welding or shielded manual arc (stick) welding.

Figure 30 shows a repair made to the inside weld deposit of the longitudinal seam in Piece T117-CE-LS-E. The repair was approximately 2 inches long. Two metallographic sections across the repaired area were made. These are shown in Figure 31 and Figure 32.

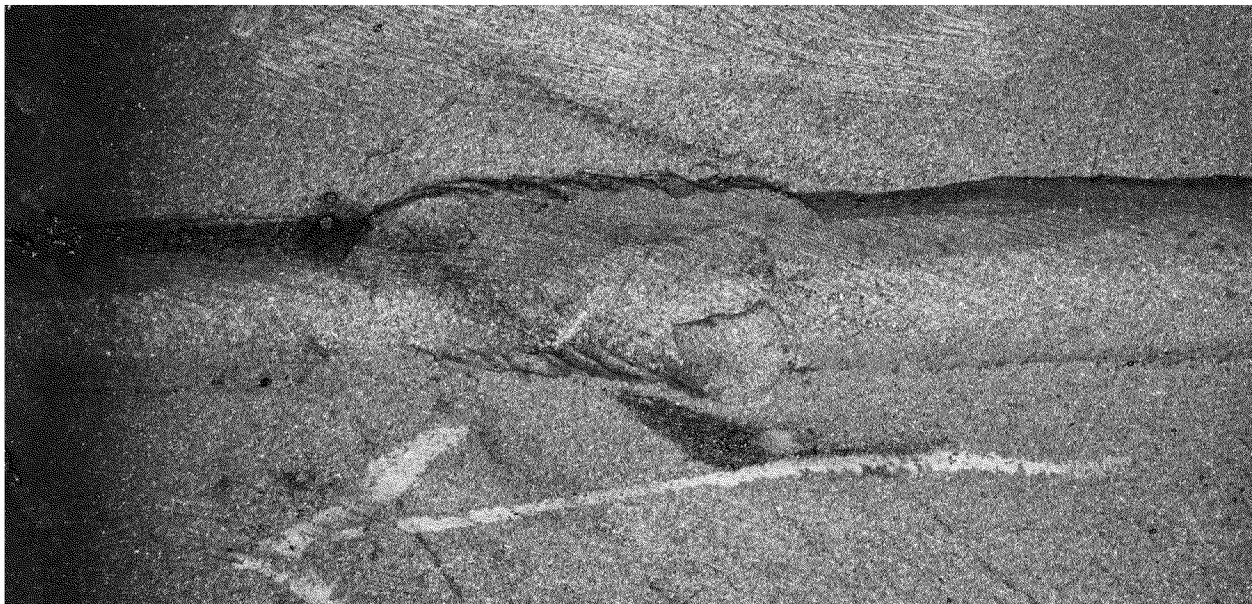


Figure 30. Seam Weld Repair, T117-CE-LS-E, Interior Surface

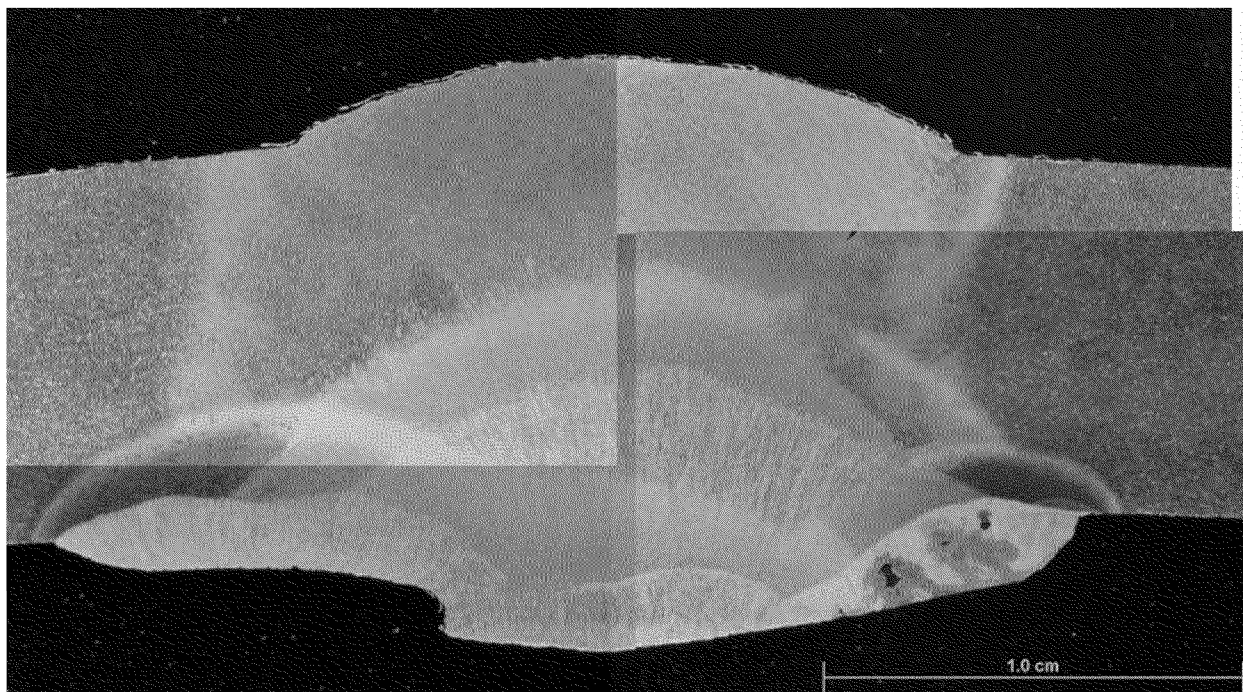


Figure 31. Seam Repair, T117-CE-LS-E, Section A

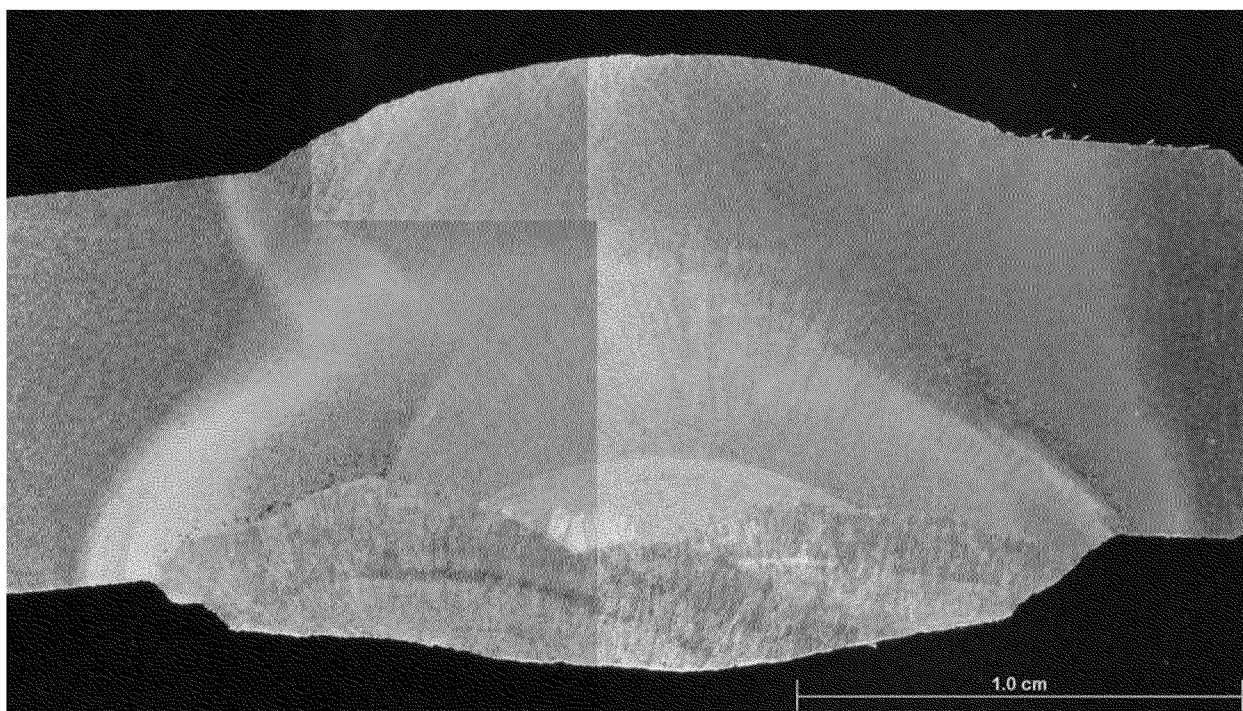


Figure 32. Seam Repair, T117-CE-LS-W, Section B

A minor repair was made at another location along the seam, shown from piece T117-CE-LS-W in Figure 33. A metallographic cross section of this area is shown in Figure 34.

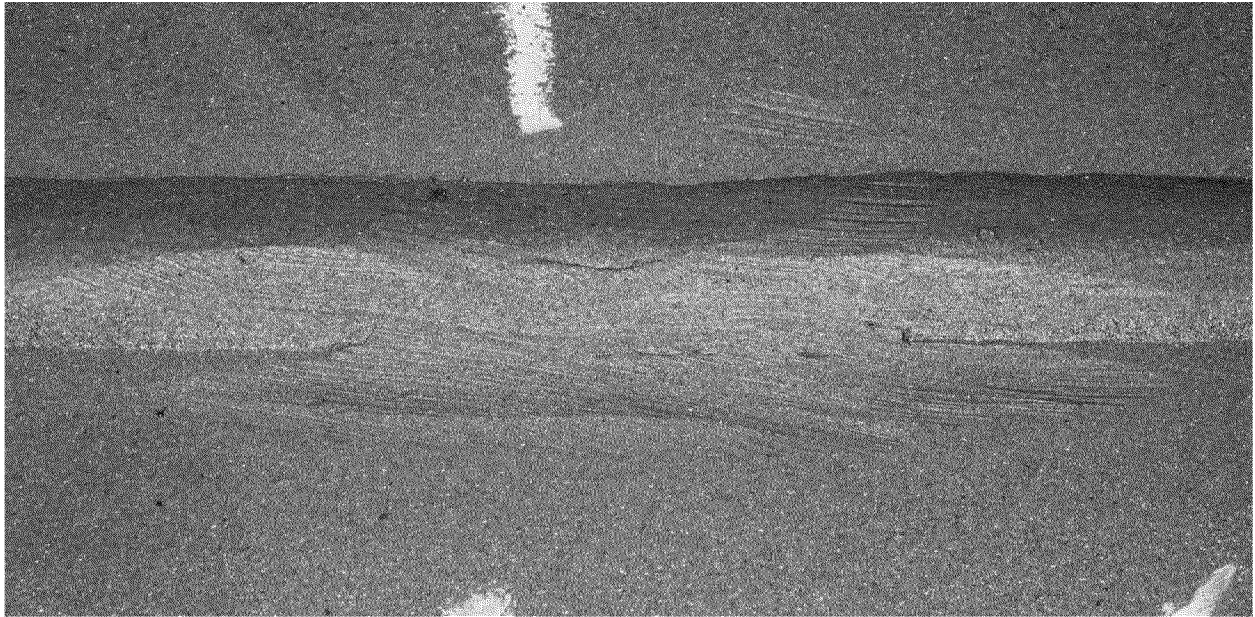


Figure 33. Seam Repair, T117-CE-LS-W, Interior Surface

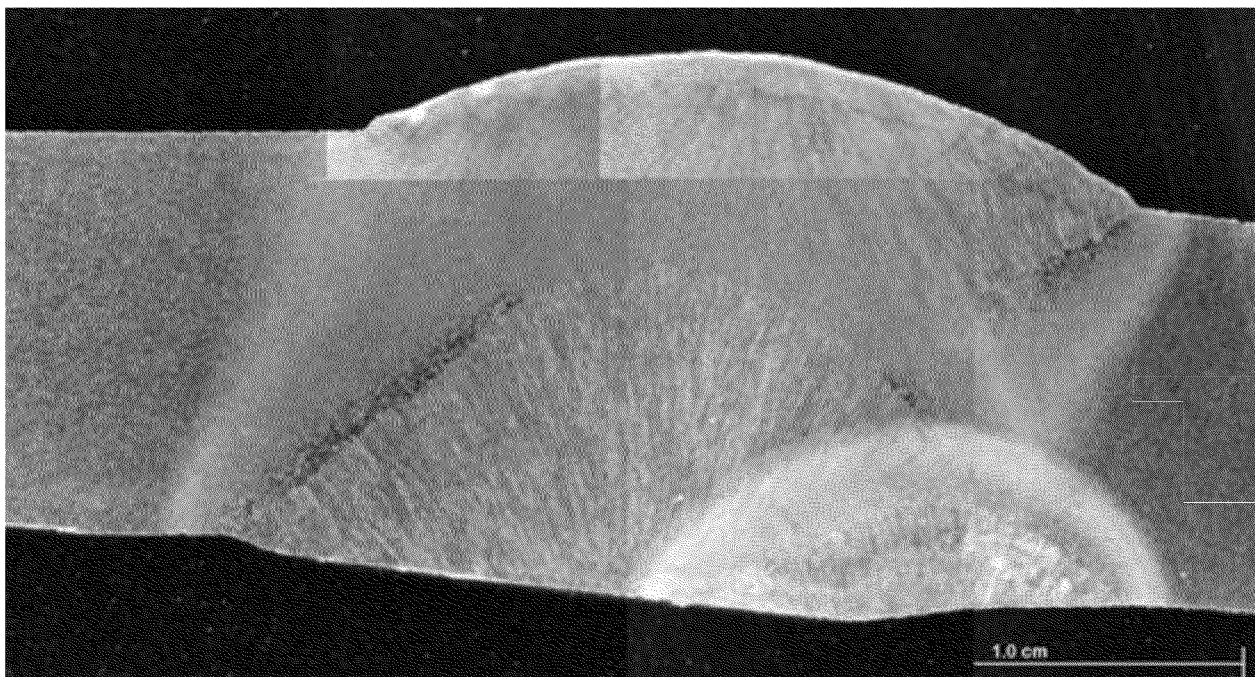


Figure 34. Seam Repair, T117-CD-LS-W, Section A

A metallographic section through an intact part of the seam in the center of the failed joint, piece T117-CC-T-W revealed a small hot crack having a radial dimension of approximately 0.12 inch (3 mm). This is shown at high magnification in Figure 35. A lack of penetration between the inner and outer weld passes and having a radial dimension of 0.02 inch (0.5 mm) was also

identified as shown in Figure 36. Neither feature was significant in terms of their effect on the integrity of the pipe.

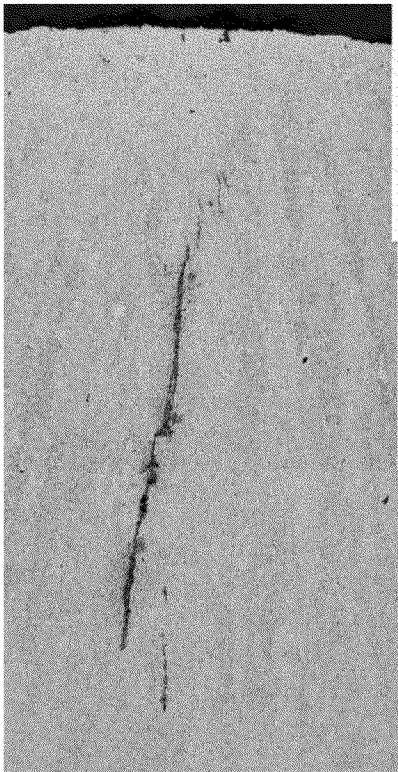


Figure 35. Hot Crack, T117-CC-T-W (25X)



Figure 36. LOP Feature, T117-CC-T-W (50X)

An indication was discovered on the exterior surface of the pipe body, shown in Figure 37 approximately actual size. It had an overall length less than ½ inch. A metallographic section established that it was a superficial blemish characterized as a surface lap. It had a depth of approximately 0.04 inch (1 mm) and was not oriented radially.



Figure 37. Surface Imperfection, T117-CE-LS-W

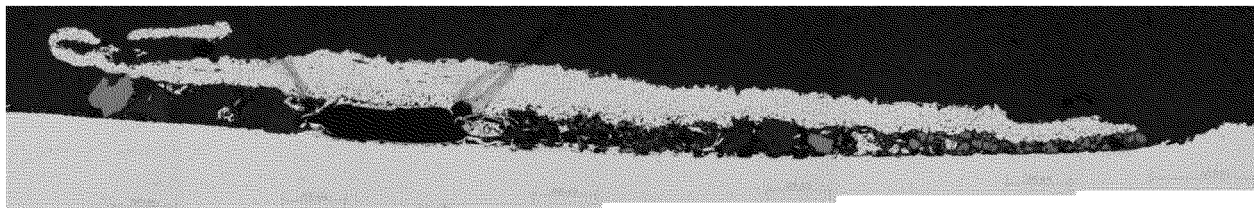


Figure 38. Surface Imperfection, Metallographic Section